

# Spectra of collective excitations of particles in normal and superfluid liquids

V.V. Brazhkin

DOI: <https://doi.org/10.3367/UFNe.2025.01.039852>

## Contents

1. Introduction	490
2. Vibrational excitations in disordered media	491
3. Superfluid helium: discovery of collective excitations	493
4. Excitation spectra in ordinary liquids I: Brillouin pseudozones and pseudorotons	494
5. Excitation spectra in ordinary liquids II: ‘Fast sound,’ shear excitations, anomalous liquids, and ‘mixing’ of longitudinal and transverse branches	495
6. Excitation spectra of superfluid and normal liquids: find five differences	498
7. Collective excitations and heat capacity of normal and superfluid liquids	502
8. Helium excitation spectrum as a key to microscopic description of superfluidity	506
9. Conclusions	509
References	510

**Abstract.** We consider the specific features of collective excitations in disordered media, mainly in liquids. We discuss the difference between proper excitations in disordered media and plane harmonic waves, and the related problem of effective excitation damping. A detailed comparative analysis of the spectra of collective excitations in normal liquids and in superfluid helium is carried out. The aspects discussed include the phonon and roton parts of the spectrum, the phenomenon of ‘fast sound,’ shear waves, and the ‘mixing in’ of longitudinal and transverse excitations in liquids. Excitations in liquids are shown to determine the thermodynamic properties in both normal and superfluid states. Despite the qualitative similarity of the spectra of superfluid helium and ordinary liquids, they show significant differences, which have not yet received a proper theoretical description in our opinion. We emphasize the major differences between superfluid helium and superfluid Bose condensates of ensembles of ultracold atoms. A hypothesis is put forward regarding the possible major role that the high zero-point energy of helium atoms at ultralow temperatures plays both in understanding the features of the excitation spectra and in the superfluidity phenomenon itself.

**Keywords:** collective excitations, liquids, superfluid helium, heat capacity

## 1. Introduction

Collective excitations of atoms and molecules in crystals are successfully described in terms of phonon spectra. Phonon excitations (plane harmonic waves) are eigenwaves of a periodic lattice of atoms or molecules with a harmonic potential of interparticle interaction. Excitation spectra in crystals, i.e., the dependences of the phonon frequency  $\omega$  on the wave vector  $\mathbf{k}$  inside the first Brillouin zone, have been effectively studied both theoretically and experimentally. Theoretical analysis typically reduces to finding the eigenvalues of the dynamical matrix (in fact, the frequencies squared), which is in turn constructed on the basis of information on the potentials of effective interparticle interaction in crystals [1]. Phonon spectra are studied experimentally using inelastic neutron scattering, and recently also using inelastic X-ray scattering. Low-frequency regions of the spectrum are also studied by ultrasound and Brillouin scattering of light. Raman scattering provides information on the frequencies of optical phonons at small wave vectors near the center of the Brillouin zone. We also note that, due to the kinematic limitation in studying the spectra by inelastic neutron scattering, the neutron speed must exceed the speed of sound in a sample under study. For a number of crystals, this condition is not satisfied, and the momentum conservation law is satisfied when the processes of transfer to one or several wave vectors of the reciprocal lattice are taken into account. The phonon branches are therefore actually studied in the second or third Brillouin zones.

In liquids and glasses, there is no translation order in the arrangement of atoms and molecules, and hence excitations in these media are obviously not ordinary phonons. It is not very clear how to describe excitations in disordered media theoretically; in the recent past, moreover, there was little hope of recording distinct spectra of collective excitations

V.V. Brazhkin

Vereshchagin Institute for High Pressure Physics,  
Russian Academy of Sciences,  
Kaluzhskoe shosse 14, 108840 Troitsk, Moscow, Russian Federation  
E-mail: [brazhkin@hphi.troitsk.ru](mailto:brazhkin@hphi.troitsk.ru)

Received 25 November 2024, revised 10 January 2025  
*Uspekhi Fizicheskikh Nauk* 195 (5) 519–542 (2025)  
Translated by S. Alekseev

experimentally. At the same time, ordinary sound waves in liquids and glasses propagate quite well, and therefore the low-frequency limit of excitations must be similar to ordinary long-wave phonons with a linear gapless spectrum  $\omega(k)$ .<sup>1</sup>

Rather amazingly, studies of the spectra of collective excitations in liquids, both theoretical and experimental, began not with ordinary liquids, but with superfluid helium 4. It is doubly amazing that the theory developed was significantly ahead of experimental studies. The phenomenon of superfluidity was discovered by Kapitza in 1938. The spectrum of excitations in superfluid helium was predicted theoretically by Landau in 1941 [2]. In 1947, Landau refined and corrected his predictions of the spectrum [4]. The first experimental spectra of excitations in superfluid helium were obtained in 1958 [5, 6]. But, until the 1980s, there were hardly any studies of excitation spectra in ordinary liquids and glasses. Due to such a large time gap, the causes for which are discussed below, studies of excitation spectra in normal and superfluid liquids are still being conducted by different scientific groups within different scientific paradigms, practically isolated from one another. This is in sharp contrast, for example, to the history of studying metals in the normal and superconducting states: studies of the transport and magnetic properties of metals in the normal state have been actively conducted since the mid-19th century; the phenomenon of superconductivity was discovered in 1911; the theory of normal metals was developed in the 1920s–1930s, and the theory of superconductivity (not finalized) was developed in the 1950s. We see that the sequence in which normal and superconducting states in metals were studied is quite natural, in contrast to the situation with the normal and superfluid states in liquids. Theoretical and experimental studies of superconductivity and the properties of metals in the normal state are carried out by the same research teams in the framework of a single scientific paradigm. We note that superconductivity is observed in dozens of elementary substances and thousands of compounds, while superfluidity in liquids is observed only in helium 4 and helium 3. There is also indirect evidence of possible superfluidity of hydrogen (in a mixture with helium). The hypothetical superfluidity (as well as superconductivity) of the matter of neutron stars [7] and the superfluidity of Bose–Einstein condensates of the ultracold gas of atoms are phenomena of a different kind, and they have no direct relation to the physics of condensed matter. In addition, superfluidity in helium 3 is observed at temperatures below 2 mK, which greatly complicates the application of many experimental techniques or merely makes it impossible. Thus, superfluid helium 4 actually remains the one and only object for studying superfluidity.

As a result, there are currently quite a few reviews devoted to the spectrum of collective excitations in liquid helium [8], and a number of monographs and reviews considering collective excitations in normal liquids [9–11]. At the same time, with few exceptions, a comparative analysis of the spectra of normal and superfluid liquids is not available in the literature. The purpose of this mini-review is to conduct such an analysis. As we see in what

follows, a detailed comparison of the spectra leads to many nontrivial conclusions about the nature of superfluidity in and of itself. In addition, a number of interesting, not yet fully resolved, issues in the physics of disordered media are to be considered.

## 2. Vibrational excitations in disordered media

Collective excitations in condensed media with strong interparticle interaction occur as coupled nonlinear oscillations [12]. At large oscillation amplitudes, some of the particles change their quasiequilibrium position, which gives rise to a diffusion component of particle motion [12]. In solids (crystals and glasses), such diffusion hops are quite rare, but the contribution of the diffusion type of particle motion in liquids is comparable to the oscillatory one [13]. We note that in any closed conservative system, including liquids and glasses, energy is conserved and the collective eigenexcitations are always undamped, by definition [14, 15]. However, the problem is that, in disordered media, these excitations are very complex coupled nonlinear oscillations that do not decouple into individual modes. Therefore, when we talk about the damping of collective excitations in liquids or glasses, we mean the attenuation of plane harmonic waves with a fixed frequency and wave vector (like phonons in crystals), and not eigenexcitations.

In experimental studies of spectra, just the response of the system to plane harmonic waves is recorded: they are acoustic waves in ultrasound studies, light waves in studies using Brillouin or Raman scattering, X-rays in studies using inelastic X-ray scattering, and de Broglie waves of neutrons in studies using inelastic neutron scattering. All of the above waves have fixed frequencies and wave vectors both before and after scattering, and hence the experimental response is actually manifested in the basis of plane harmonic collective excitations, which are not eigenexcitations of a disordered system and decay in a finite time. This decay time, being the time of ‘affinity’ of an eigenexcitation to a plane harmonic wave, is precisely what is recorded in the experiment. For example, in studies using inelastic neutron and X-ray scattering, the decay is determined from the width of the corresponding peaks of the dynamical structure factor. Theoretical analyses of excitation spectra typically involve the basis of plane harmonic waves, and their damping in disordered media is then analyzed.

Crystals have a translation order, and hence the wave vector  $\mathbf{k}$  is a ‘good’ quantum number for the excitation quanta (phonons) meaning that plane waves are eigenexcitations. At low temperatures and small amplitudes of atomic oscillations, these oscillations are almost harmonic, i.e., the frequency  $\omega$  is also a ‘good’ quantum number for phonons. As a result, plane harmonic excitations in crystals are actually eigenexcitations and are weakly damped. The corresponding phonon spectrum (the dependence  $\omega(k)$ ) also experiences almost no damping. As the temperature increases, the oscillation amplitude increases and the anharmonicity of the potential starts having an effect. The phonon frequency  $\omega$  ceases to be a ‘good’ number, and phonons start being damped, which is described in terms of multiphonon processes [16] (Fig. 1a).

In disordered media, there is no translation order, the wave vector  $\mathbf{k}$  is a ‘bad’ number, and plane waves are not eigenexcitations at any temperature. At the same time, oscillations are almost harmonic at low temperatures, and

<sup>1</sup> Interestingly, Landau drew attention to this rather trivial fact in his first paper devoted to the theory of superfluidity of helium 4 [2], where, in particular, he discussed errors in Bijl’s paper [3]. Bijl assumed that there should be a gap in the excitation spectrum of liquid helium, with gapless excitations absent altogether.

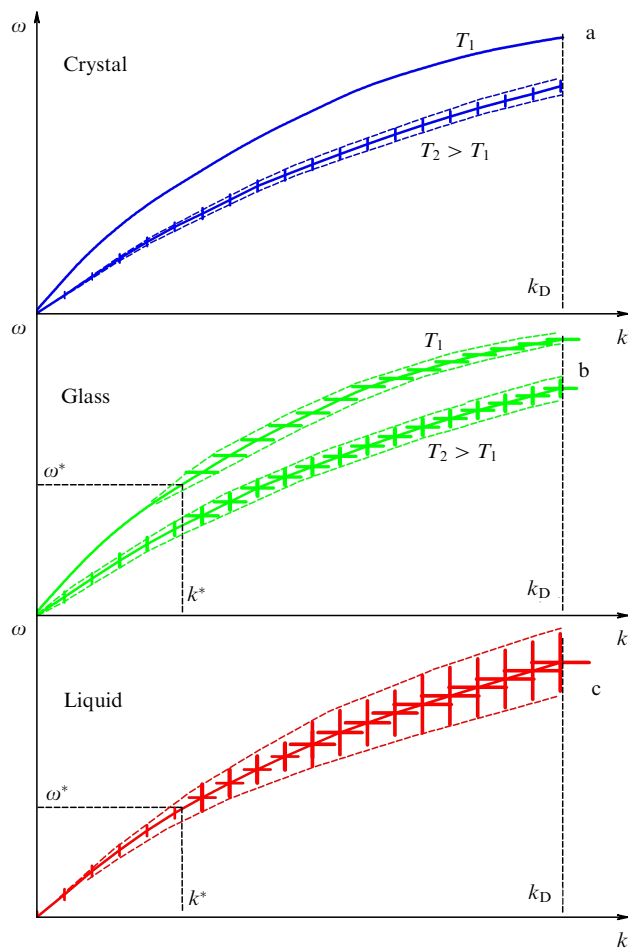


**Figure 1.** Qualitative behavior of spectra of collective excitations (phonons)  $\omega(k)$  for (a) crystals, (b) glasses, and (c) liquids. Vertical and horizontal segments show effective damping of excitations, respectively associated with anharmonicity and absence of translation order.  $k_D$  is maximum wave vector corresponding to boundary of Brillouin zone or pseudozone,  $k^*$  is wave vector corresponding to wavelength comparable to intermediate order scale in the glass or liquid, and  $\omega^*$  is excitation frequency corresponding to wave vector  $k^*$ .

we actually face a standard problem from theoretical mechanics, where  $3N$  eigenfrequencies of oscillations occur in a harmonic system of  $N$  particles. Unlike crystals, eigenexcitations in such glasses are complex combinations of oscillations with different frequencies, which do not decouple into individual modes. However, at wavelengths longer than the structural inhomogeneity scale in the glass (in fact, the intermediate-order scale of 3 to 5 interparticle distances), the waves do not ‘feel’ disorder. Plane waves with small wave vectors are therefore eigenexcitations of a continuous medium. Such waves have very weak Rayleigh-type damping ( $\sim \omega^4$ ). This is so for wave vectors  $k < (0.2-0.3)k_D$ , where  $k_D$  is the maximum possible wave vector of the order of  $\pi/a$ , where  $a$  is the average interparticle distance (the pseudo-Brillouin zone boundary). Notably, this is true for ordinary sound waves. At shorter wavelengths, the  $k$  vectors become ‘bad’ wave numbers, which results in strong effective phonon damping (Fig. 1b). As the temperature increases, anharmonicity effects ‘turn on’ in both glasses and crystals, and the frequency  $\omega$  also becomes a ‘bad’ number, leading to additional effective phonon damping (Fig. 1b).

In liquids, due to the large amplitude of oscillations, anharmonicity effects are always significant. At the same

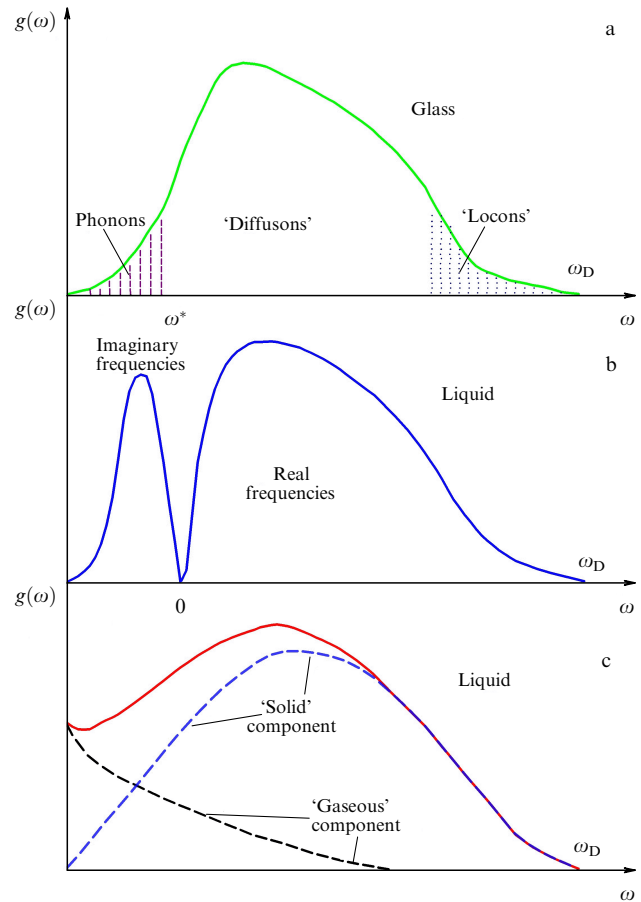


**Figure 2.** Qualitative behavior of density of states of collective excitations  $g(\omega)$  (a) in glasses [18], (b) in liquids within the instantaneous mode approach [19], and (c) in liquids with separation into gas and solid components according to [20].

time, at small wave vectors, as in glasses, the eigenexcitations are almost plane waves, and sound vibrations propagate with only little damping (Fig. 1c). At small wavelengths, the effective damping of phonons in normal liquids is always very large. Furthermore, in addition to oscillatory motion, a significant part of particles in liquids also experience diffusion hops, which also leads to an increase in the effective damping of excitations. The fact that plane waves are not eigenwaves at small wavelengths in disordered systems has one more important consequence: the mixing of longitudinal and transverse excitations. We discuss this important point in Section 5.

Because the wave number  $k$  is ‘bad’ for most excitations of disordered media and the damping may not be very large due to anharmonicity, it follows that it is more appropriate in many cases not to consider the dispersion curves  $\omega(k)$  but the density of states of collective excitations  $g(\omega)$ , which shows how many excitations are in the corresponding frequency range or, more generally, in the energy range (Fig. 2). In glasses at low frequencies (corresponding to long wavelengths), as noted above, the eigenexcitations are almost ‘normal’ phonons. An additional increase in the density of phonon states compared to crystals, called the boson peak [17], also occurs in glasses at low frequencies; a discussion of the boson peak is beyond the scope of this review. At higher frequencies corresponding to shorter wavelengths, the eigenexcitations are very different from plane waves, and are sometimes called diffusons [18] (Fig. 2a). In particular, just

the diffusons determine low thermal conductivity in glasses compared to crystals. We recall that crystals without phonon anharmonicity would have infinite thermal conductivity. The situation is quite similar to the picture of electron Bloch waves in metals, where a crystal without defects must have infinite electrical conductivity (zero resistance) at zero temperature. In metallic glasses, electrons are no longer plane Bloch waves, and the conductivity remains finite at any temperature. In the high-frequency range, some of the excitations in glasses can be localized in small spatial regions, and the term ‘locons’ is sometimes used for them (Fig. 2a).

When analyzing the density of states of excitations in a liquid, an additional complication arises due to the large weight of nonoscillatory diffusion processes. Theoretical calculations are typically based on two alternative approaches. In the first, for an instantaneous configuration of liquid particles in a computer simulation, the force and dynamical matrices and the squares of eigenfrequencies of oscillations are calculated in the harmonic approximation (the approach of ‘instantaneous modes’) [19]. In contrast to crystals and glasses, a significant number of the dynamical matrix eigenvalues (squares of eigenfrequencies) turn out to be negative, and the frequencies are therefore imaginary. Imaginary frequencies correspond to unstable particle configurations, which are precisely what generates diffusion hops. Part of the density of states with imaginary frequencies is conventionally represented on the negative axis (Fig. 2b). We note that, with strong anharmonicity of oscillations in solids, imaginary modes also occur within this approach, which in many ways denigrates this concept itself. In addition, as already noted by Landau, imaginary frequencies formally correspond to exponentially decaying and exponentially increasing solutions, which leads to a violation of the energy conservation law.

In another approach, where no harmonic excitations are assumed, the density of states is calculated as the Fourier integral of the autocorrelation function of particle velocities [20]. This approach can be applied equally well to both solids and gases, and the resulting density of states simply reflects the fraction of excitations with a certain energy. Because excitations can be anharmonic in this approach, the density of states remains finite at zero frequency, in contrast to the model of ‘instantaneous modes.’ The density of states of excitations for a liquid obtained in this approach can be conventionally divided into a nearly harmonic ‘solid-like’ part and a totally anharmonic ‘gas-like’ part (Fig. 2c).

We note that the density of states of collective excitations in dielectric liquids and glasses uniquely determines the thermodynamic properties, including heat capacity (see Section 7).

In summary, we can conclude that excitations in a normal liquid, due to the absence of translation order, are very different from plane harmonic waves, and excitation spectra have to exhibit strong effective damping, which must dramatically increase for large wave vectors  $k > 0.2\text{--}0.3$   $k_D$ . Such behavior should not be strongly dependent on temperature and should be observed down to zero temperatures in both glasses and liquids. At the same time, we note that, unlike glasses, liquids in a stable state are in thermodynamic equilibrium, and their entropy must tend to zero at low temperatures. At first glance, this should indicate the manifestation of some order in liquids. We consider this issue in more detail in Section 7.

### 3. Superfluid helium: discovery of collective excitations

The history of the study of helium superfluidity has been the subject of many reviews and monographs [21–23], and we only recall the main points briefly. The superfluidity of liquid helium, i.e., its ability to flow without friction through narrow gaps and to rise along the walls of vessels at temperatures below the  $\lambda$ -point (2.17 K), was discovered and intensively studied in Kapitza’s laboratory in 1938, when there was not even the slightest idea about any excitation spectra in liquids. Even for crystals, the concept of a phonon as a quantum of collective excitations, proposed by I.E. Tamm and Ya.I. Frenkel in the early 1930s, had not yet become universally accepted. Therefore, superfluid helium, partly by chance, became the first liquid whose excitation spectrum was discussed and studied. In 1941, Landau [2] suggested the presence of a linear gapless part in the  $\omega(k)$  spectrum to explain the superfluidity of helium, which is consistent with the presence of sound waves in the long-wave limit. If the motion of helium atoms is somehow correlated, such a spectrum can lead to superfluidity at fluid velocities lower than the slope of the  $\omega(k)$  spectrum line (in fact, lower than the speed of sound) [2]. In a two-fluid phenomenological model proposed for helium, it was considered to consist of a ‘normal’ and a superfluid component. The latter arises at temperatures below the point of the phase transition to the superfluid state (2.17 K), its fraction increases with a further decrease in temperature, and the fraction of the normal component becomes negligibly small at  $T < 1$  K. In addition to the linear gapless branch of the spectrum, Landau also hypothesized the presence of a quadratic part of the spectrum with a gap at the zero wave vector. This part of the spectrum, according to Landau, was responsible for the excitations of vortices of the atomic scale, rotons. Subsequently, Landau revised his views and in his 1947 paper [4] proposed a new version of the spectrum of collective excitations in superfluid liquid helium (Fig. 3a). Roton vortex excitations with a gap at the zero wave vector are absent in this spectrum, and the maximum and minimum in the  $\omega(k)$  dependence at larger  $k$  are simply a natural continuation of the linear ‘phonon’ part. Excitations in the vicinity of the minimum at a finite wave vector were also called rotons, which introduces some confusion, because this part of the spectrum is unrelated to vortex excitations. Therefore, ‘roton’ became the term for this part of the spectrum rather accidentally. Also, this roton minimum is unrelated to the nature of superfluidity; Landau decided that the presence of such a part of the spectrum was only necessary for explaining the temperature dependence of the heat capacity of helium [4].

The first experiments on inelastic neutron scattering in superfluid helium were carried out only 10 years later, in the late 1950s [5, 6, 24]. Agreement between the obtained spectra of collective excitations and Landau’s predictions was very good (Fig. 3b), which largely served as the basis for awarding Landau the Nobel Prize in 1962. Also in the 1950s, experimental studies of excitation spectra for ordinary liquids and glasses began. However, for most liquids and glasses, due to the kinematic limitations discussed above, the spectra could only be studied at large wave vectors, where very strong damping was expected. Indeed, no excitation branches were detected in normal liquids, and it took another 10 years to record strongly damped collective excitations in a number of liquid metals in a certain range of wave vectors [25] (Fig. 4a). For other simple

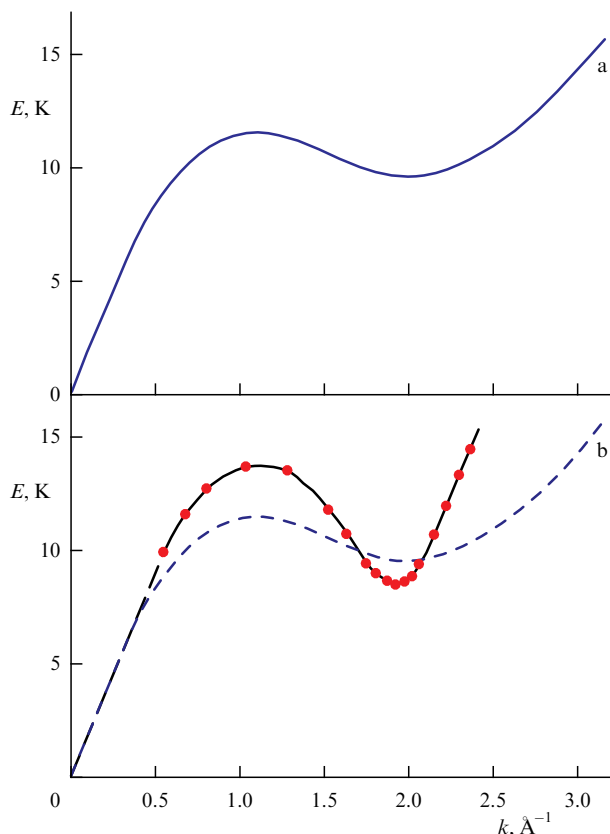


**Figure 3.** (a) Excitation spectrum in superfluid helium proposed by Landau in [4]; (b) experimental excitation spectrum in helium obtained by inelastic neutron scattering [24]. Experimental points are shown with red circles. Line is roughly drawn for convenience. Spectrum proposed by Landau (dashed line) is shown for comparison.

liquids such as argon, spectra could not be recorded at that time [26], and the scientific community in the late 1960s divided liquids into almost harmonic ones, in which collective excitations are present even if strongly damped, and ‘anharmonic’ ones, where quasiphonon branches are not observed at all. With the development of neutron experimental technology, the sensitivity of measurements increased, and, after another 20 years, strongly damped spectra were recorded for such an important liquid as water (Fig. 4b) [27]. Thus, 30 years of neutron research apparently demonstrated zero similarity between the spectra of superfluid helium and normal liquids: instead of a well-defined  $\omega(k)$  dependence in a wide range of wave vectors, which was the case for helium, only very smeared parts of the spectra in a limited range of wave vectors were observed for normal liquids.

#### 4. Excitation spectra in ordinary liquids I: Brillouin pseudozones and pseudorotons

The situation changed dramatically by the beginning of the 21st century. Due to the appearance of powerful third-generation synchrotron sources, a method for studying collective excitations in condensed media using inelastic X-ray scattering was developed. There is no ‘kinematic limitation’ for this method, and spectra can be studied in almost the entire range of wave vectors. Neutron research techniques also progressed rapidly in terms of both the power of neutron sources and the sensitivity and resolution of detectors. As a result, the study of collective excitation

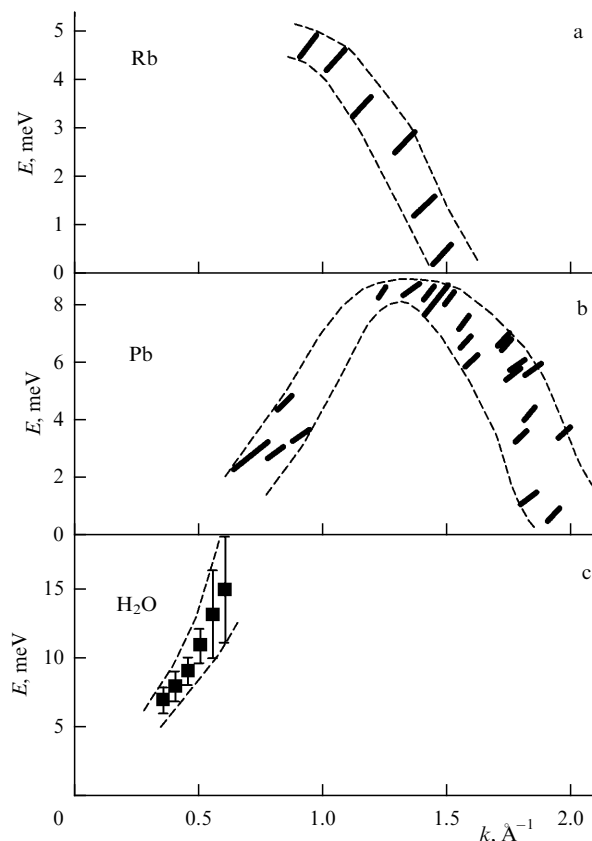


**Figure 4.** Experimental spectra of collective excitations obtained by inelastic neutron scattering for (a) rubidium and (b) lead melts according to [25]; (c) experimental excitation spectrum obtained by inelastic neutron scattering for water [27]. Experimental points are shown with smearing (damping) of spectra taken into account. Lines are roughly drawn for convenience.

spectra in liquids and glasses went from a marginal to a respectable area of physics in its own right. A number of reviews have been written on this subject, including [10, 28], and we therefore present only the main results in Sections 4 and 5. It turns out that the spectra of different classes of liquids are qualitatively very similar to each other. Dissimilar liquids such as inert gas fluids (Fig. 5), alkali metal melts (Fig. 6), and liquid semiconductors and semimetals (Fig. 7) have the same characteristic spectral features. After the quasilinear phonon part of the spectrum, the  $\omega(k)$  dependence flattens, which is followed by a maximum and a minimum; qualitatively, therefore, all spectra are similar to that of superfluid helium as long as we disregard the magnitude of damping. Consequently, at first glance, all liquids (as well as glasses!) exhibit phonon and roton excitation modes. Moreover, studies of the spectra at long wave vectors have shown the presence of subsequent maxima and minima, approximately equidistant from each other (Figs 5a, 6b, and 7a–c). For larger wave vectors, the maxima and minima become less pronounced, and the spectra of collective excitations smoothly pass at high energies into almost linear spectra of single-particle excitations [10]. We note that the problem of large effective damping of the spectra, which was discussed in the preceding sections, has certainly not gone away. Relatively small damping is indeed observed experimentally only for small wave vectors  $k < (0.2\text{--}0.3)k_D$ ; for large wave vectors, the damping increases and becomes comparable in magnitude to the

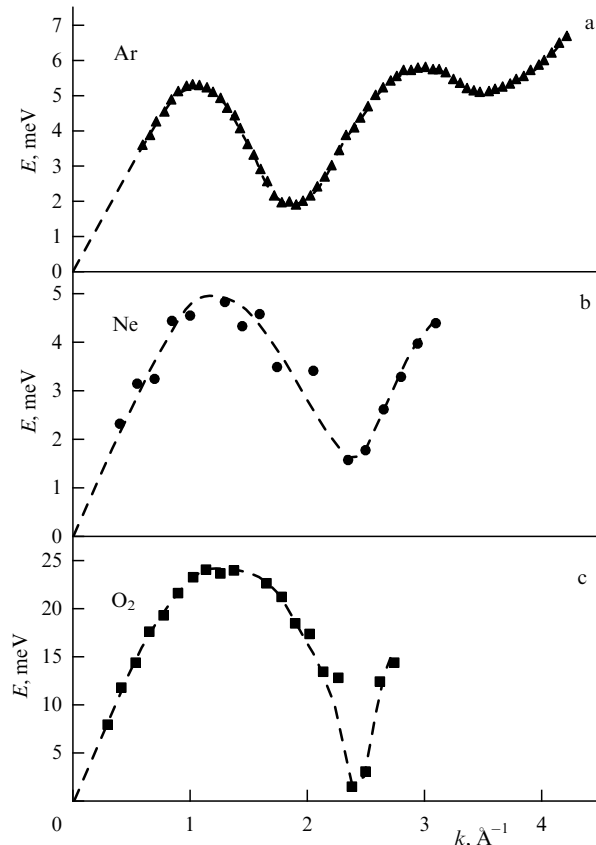


**Figure 5.** Experimental spectra of collective excitations in liquefied gases obtained by inelastic X-ray scattering. Experimental points are shown for (a) argon [29], (b) neon [30], and (c) oxygen [31]. Excitation energies for oxygen are high, because spectra were obtained for fluid at ultrahigh pressures. Lines are roughly drawn for convenience. Damping is not shown; for all fluids, it is large and comparable in magnitude to frequency for large wave vectors starting from second Brillouin pseudozone.

frequency. Amazingly, the striking similarity of the spectra of collective excitations of normal liquids and superfluid helium is hardly discussed at all; as noted above, the interests of scientists in these two research fields have greatly diverged over the past 70 years.

In all cases, subsequent maxima and minima in the spectra were distanced from the preceding ones by a wave vector close to the one for the main peak of the static structure factor, which immediately allows drawing an analogy with crystals, as was indeed done in [35]. In crystals, the phonon excitation spectra in the scheme of repeating Brillouin zones are a repeating collection of dome-shaped sections (Fig. 8a). In liquids, there is a similar picture of repeating Brillouin pseudozones, but, due to the presence of disorder, the boundaries of the pseudozones are blurred and the wave vector of the reciprocal lattice is also defined up to some error (Fig. 8b) [35]. Starting from the second pseudozone, the dependence  $\omega(k)$  no longer touches zero, but passes through increasingly shallow minima and after 4 to 5 oscillations reaches a line corresponding to the ballistic motion of individual particles (Fig. 5a) [10].

Thus, the parts of the excitation spectra in liquids in the vicinity (vicinities) of the minima are not some specific roton excitations but blurred ‘duplicates’ of real excitations near the zero wave vector. We note that, in polycrystals, due to the mismatch between the wave vectors at the boundaries of the Brillouin zone for different crystallographic directions, a kind

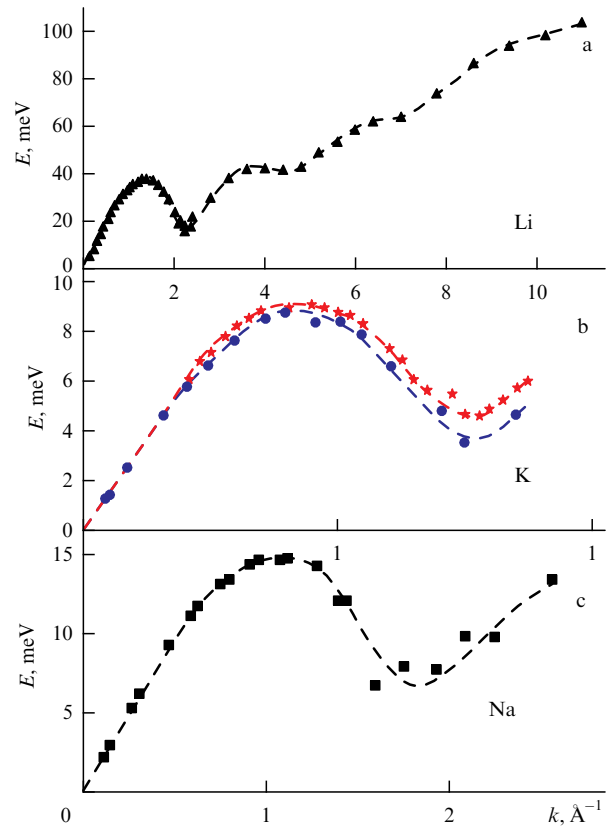


**Figure 6.** Experimental spectra of collective excitations for metal melts obtained by inelastic X-ray scattering. Experimental points are shown for (a) lithium [10], (b) potassium [10], and (c) sodium [32]. For potassium, data obtained by inelastic neutron scattering are also shown (asterisks). Lines are roughly drawn for convenience. Damping is not shown; for all fluids, it is large and comparable in magnitude to frequency for large wave vectors starting from second Brillouin pseudozone.

of effective blurring of the zone boundaries occurs, and the spectra are also blurred. The  $\omega(k)$  dependence does not touch the zero frequency at the boundary of the second zone either and passes through a pseudoroton minimum (Fig. 9a) [32]. The first conclusion about the similarity of excitation spectra in polycrystals and disordered systems seems to have been made in [36], where the excitation spectrum of glass consisting of identical particles with the Lennard-Jones potential was obtained by computer simulations (Fig. 9b). Therefore, pseudorotons in liquids and glasses with wave vectors near the boundary of the second Brillouin pseudozone are not real excitations. To calculate the thermodynamic properties, including heat capacity, we must take only the real part of the spectra inside the first Brillouin pseudozone, with its blurring taken into account. All of the above, at first glance, casts doubt on the reality of the roton part of the spectrum in superfluid helium. Does it turn out that Landau predicted nothing interesting or new? We return to this issue in Section 6.

## 5. Excitation spectra in ordinary liquids II: ‘fast sound,’ shear excitations, anomalous liquids, and ‘mixing’ of longitudinal and transverse branches

Another striking feature in the study of excitation spectra in liquids was discovered using inelastic X-ray scattering: the

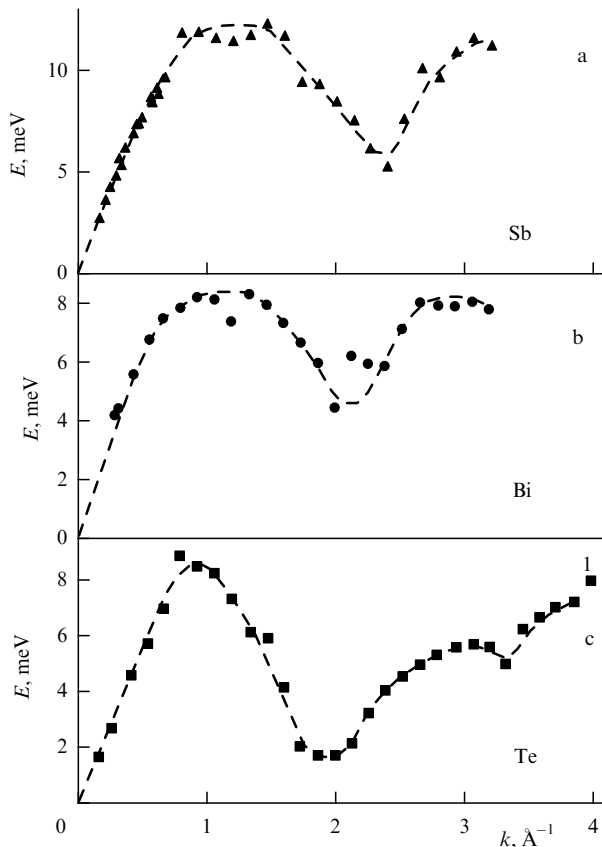


**Figure 7.** Experimental spectra of collective excitations for semiconducting and semimetal melts obtained by inelastic X-ray scattering. Experimental points are shown for (a) antimony [33], (b) bismuth [33], and (c) tellurium [34]. Lines are roughly drawn for convenience. Damping is not shown; for all fluids, it is large and comparable in magnitude to frequency for large wave vectors, starting from second Brillouin pseudozone.

presence of positive dispersion of sound (deviation from the linear dependence  $\omega(k)$  starting from a finite-magnitude wave vector) [10, 37]. Later, the term ‘fast sound’ was assigned to this phenomenon (despite the fact that the same term was previously used to describe sound waves in gas mixtures). One of the first and most lucid examples of ‘fast sound’ is the spectrum of collective excitations in water [38] (Fig. 10). For wave vectors  $k > 0.01 \text{ \AA}^{-1}$ , a significant upward deviation from the linear dependence is observed, meaning that the speed of sound at high frequencies and large wave vectors significantly exceeds the speed of sound in the hydrodynamic long-wave limit. In recent years, the ‘fast sound’ phenomenon has been discovered and studied in dozens of different liquids [38].

Also recently, transverse sound excitations have been discovered at high frequencies, first for model systems, and, with the increase in measurement sensitivity, also in real liquids (see [38] and the references therein). These shear excitations propagate in liquids only starting from a certain finite wave vector; in other words, there is a gap in the wave-vector dependence ( $K$ -gap) of the transverse branch of excitations in the spectrum [11, 38]. The wave-vector gap increases as the temperature increases and can extend to the entire first Brillouin pseudozone. In this case, quasi-harmonic shear excitations in the liquid disappear at all eigenfrequencies and a transition from liquid to quasigas occurs on the so-called Frenkel line [13, 39, 40].

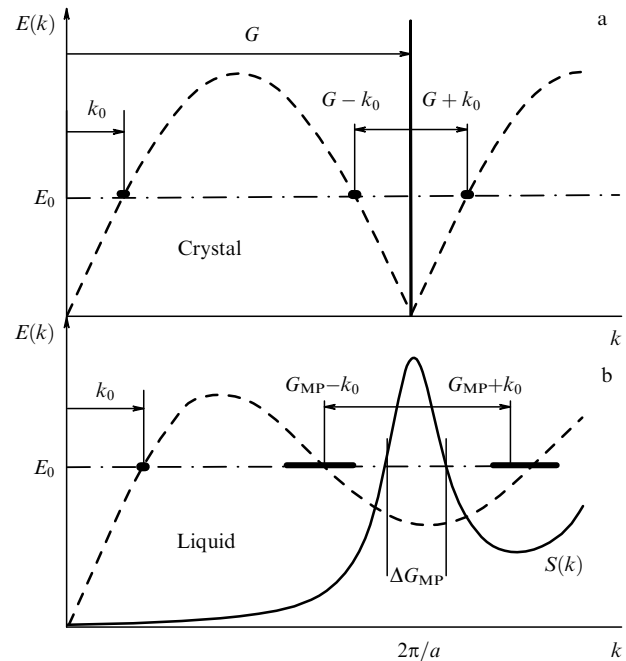


**Figure 8.** Qualitative picture of spectra of collective excitations in (a) crystals and (b) liquids according to [35] in scheme of repeating Brillouin zones for crystals and pseudozones for liquids.  $G = 2\pi/a$  is wave vector of reciprocal lattice for the crystal, where  $a$  is interatomic distance, and  $G_{MP}$  is wave vector corresponding to position of main peak of static structure factor  $S(k)$  (reciprocal pseudolattice vector):  $G_{MP} \approx 2\pi/a$ , where  $a$  is average interparticle distance in the liquid. Phonons for a crystal with energy  $E_0$  and wave vectors  $k_0$ ,  $G - k_0$ , and  $G + k_0$  are equivalent. Similar excitations in liquid coincide up to smearing of boundary of Brillouin pseudozone  $\Delta G_{MP}$ .

Within the standard viscoelastic model, the appearance of a transverse branch of excitations at large wave vectors must automatically lead to the appearance of ‘fast’ sound [11, 38]. Indeed, for a medium with a nonzero shear modulus, the longitudinal sound speed  $V_l$  is given by  $V_l = [(B + (4/3)G)/\rho]^{1/2}$ , where  $B$  is the adiabatic bulk modulus,  $G$  is the shear modulus, and  $\rho$  is the density of the substance. The transverse sound speed is  $V_t = (G/\rho)^{1/2}$ . At the same time, at low frequencies, the hydrodynamic speed of sound is  $V_h = (B/\rho)^{1/2}$ . The factor capturing the increase in the speed of fast sound compared to normal sound must be  $V_l/V_h = (1 + 4G/3B)^{1/2}$  [38]. We have established that taking transverse excitations into account does indeed correctly describe the scale of ‘fast’ sound for many liquids [38] (Fig. 11). An expression well known from elasticity theory predicts the magnitude of fast sound quite accurately both in model systems and in all real melts, where shear excitations at high frequencies can be recorded relatively reliably [38]. Positive dispersion of longitudinal sound (excess of velocity over hydrodynamic velocity) starts at the same wave vectors where shear excitations appear. The factor of excess ‘fast’ sound velocity over hydrodynamic velocity  $V_l/V_h$  is 1.15–1.2 for liquid metals and model systems and 1.3–1.4 for semimetallic and semiconducting melts. Accordingly, the ratio of the moduli  $G/B$  has quite normal values in the range of 0.2–0.7.

At the same time, for a number of melts, the excess of the ‘fast’ sound velocity over hydrodynamic velocity is anomalously large. Such liquids are also often called anomalous. For example, for water, the increase factor for the speed of



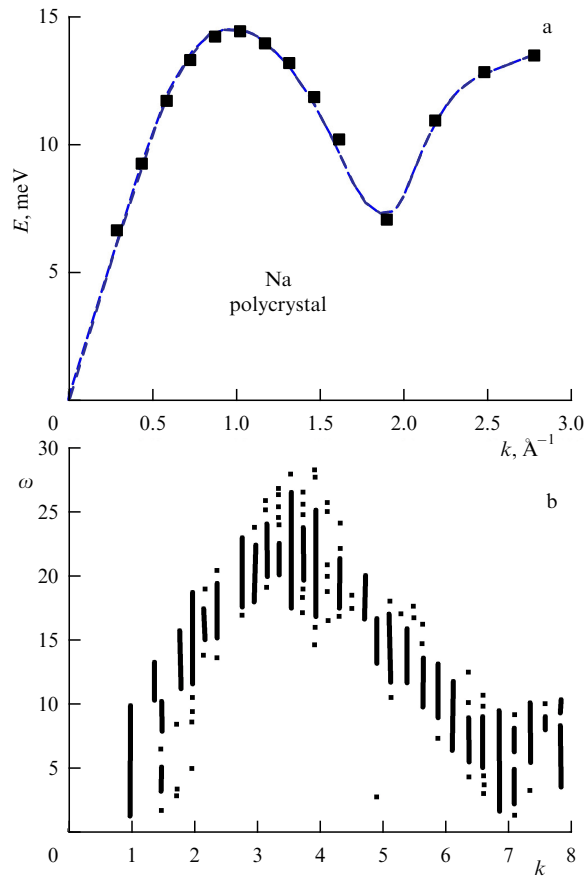


**Figure 9.** (a) Experimental spectrum of collective excitations for sodium polycrystal obtained by inelastic X-ray scattering [32]. Line is roughly drawn for convenience. (b) Spectrum of collective excitations of Lennard-Jones glass obtained by computer simulation [36]. Vertical segments correspond to damping of excitations. Units on frequency and wave vector scales correspond to data of computer experiment in [36].

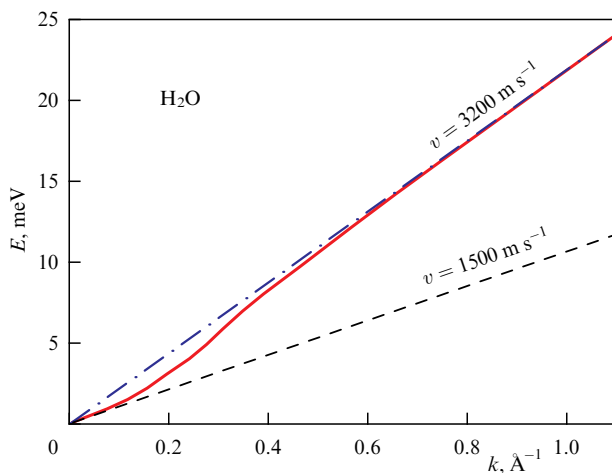


**Figure 10.** Spectrum of collective excitations in water (red line), demonstrating large positive dispersion of longitudinal excitations. Dashed line corresponds to hydrodynamic speed of sound in water in long-wave limit, and dotted line shows phase velocity of longitudinal waves at high frequencies, ‘fast sound’ [38].

‘fast’ sound is 2.1. An anomalously large increase in the speed of sound at high frequencies was also observed for molten tellurium and its compounds and molten mercury near the liquid–gas critical point (Fig. 12) [38].

As we have established, the cause of such an anomalous increase factor for the speed of ‘fast sound’ is the strong frequency dependence of the bulk compression modulus  $B(\omega)$  (its anomalous decrease at low frequencies) [38]. The correct expression for the longitudinal speed of sound must take the frequency dependence of the moduli into account:  $V_l(\omega) = [(B(\omega) + 4/3G(\omega))/\rho]^{1/2}$ . The strong frequency dependence of the bulk compression modulus is in turn associated with relaxation processes during diffuse phase transformations in water, molten tellurium, and many of its compounds, and with critical fluctuations in fluid mercury in the vicinity of the critical point. Thus, the cause of the record-breaking difference between the velocities of ‘fast’ and ‘normal’ sound in anomalous liquids is not the anomalously large ‘fast’ sound but the anomalous ‘slowness’ of ‘hydrodynamic’ sound in such liquids, where the bulk compression moduli are anomalously small at low frequencies [38].

As noted above, excitations in liquids and glasses are not plane waves at large wave vectors, and hence purely longitudinal and transverse excitations cannot be distinguished; they are ‘mixed.’ In recent years, this problem has been recognized in calculating the elastic moduli of glasses, and even a special term has emerged: ‘nonaffine dynamics of a disordered network’ [41]. In glasses, in contrast to crystals, shear stresses applied to a small region of the network inevitably lead to uncompensated forces acting on the particles inside this region, the appearance of compressive stresses, and the displacement of particles to new equilibrium positions (Fig. 13). Similarly, bulk compression of a region of a disordered network leads to the appearance of local shear stresses inside this region.

In liquids, due to disorder, an external longitudinal wave with a large wave vector inevitably generates a transverse component, and vice versa. This is illustrated in Fig. 14, which shows the data of first-principle calculations of the correlation functions of transverse and longitudinal flows for an Sn melt [42]. It is evident that each correlation function contains both components.

In fact, it is precisely due to the ‘nonorthogonality’ and ‘mixing’ of longitudinal and transverse waves in disordered media that the spectrum of shear excitations can be observed experimentally (see Fig. 11). The geometry of inelastic X-ray scattering experiments is such that, at first glance, only satellite wings corresponding to longitudinal excitations must be present in the dynamical structure factor [10]. However, due to the mixing of longitudinal and transverse waves at high frequencies, weak satellite peaks from shear excitations can also be observed in experiment. The ‘mixing’ of longitudinal and transverse branches of excitations complicates the theoretical analysis of the spectra obtained by computer simulations (Fig. 15).

Most researchers typically construct spectra based on the position of the maxima of the correlation functions of transverse and longitudinal flows, but this leads to incorrect results at large wave vectors. To obtain correct results, the correlation functions must be processed together [43]. In addition to false intersections of the branches of the spectra in the second and subsequent Brillouin pseudozones, in incorrect analysis parasitic branches appear starting from the second pseudozone [44–46]. In crystals with one atom in the unit cell, there are three phonon branches: one longitudinal and two transverse. In glasses and liquids, due to spherical



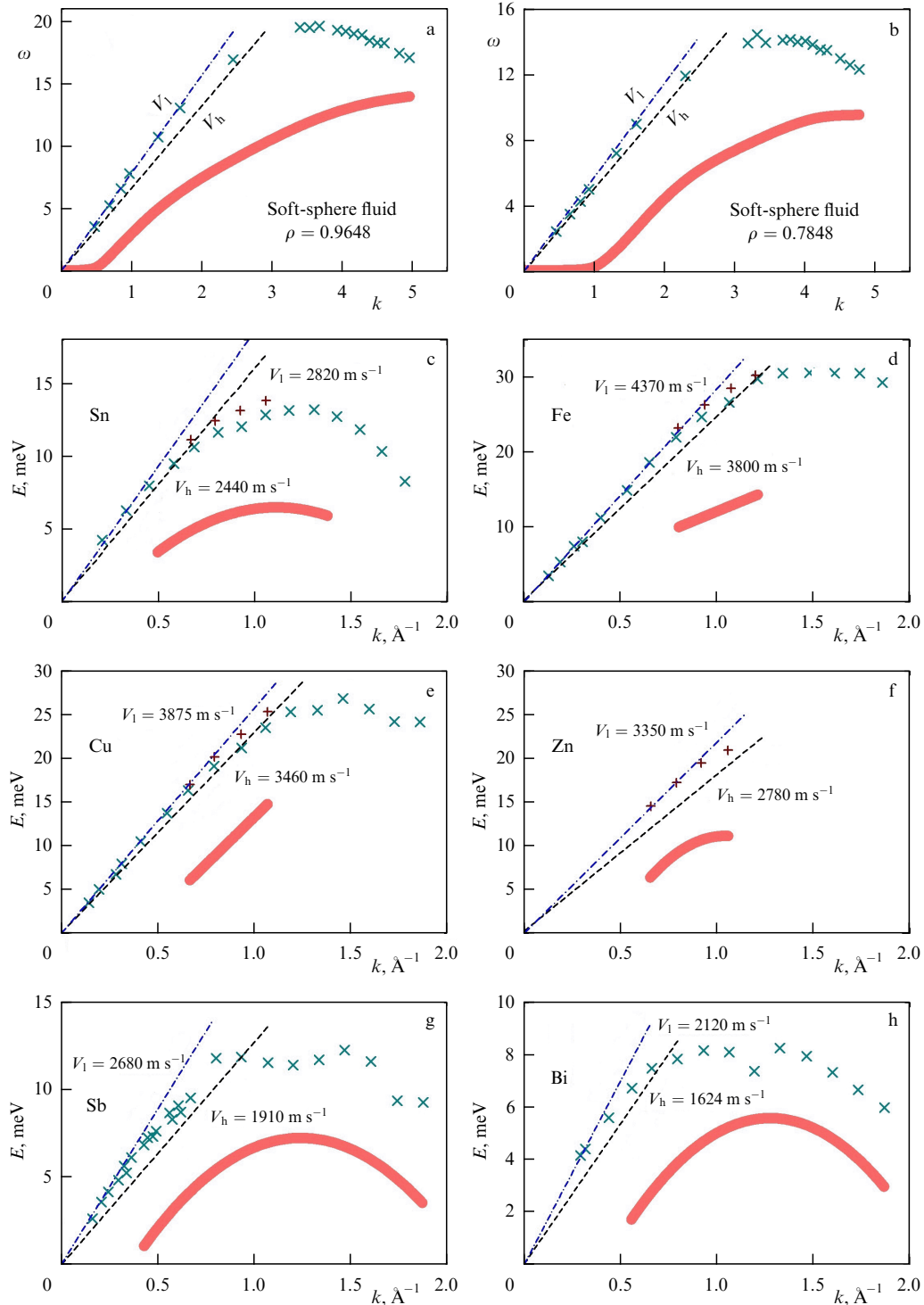


**Figure 11.** Spectra of longitudinal and transverse excitations in model systems and melts of elementary substances [38]. (a, b) Fluid of soft spheres with different densities and melts of (c) tin, (d) iron, (e) copper, (f) zinc, (g) antimony, and (h) bismuth. Thick red lines show smoothed spectra of transverse excitations. Crosses are experimental points for spectra of longitudinal excitations. Dashed lines correspond to hydrodynamic speeds of sound. Dashed-dotted lines correspond to velocities of longitudinal waves at high frequencies ('fast sound'), calculated using formula  $V_l^2 = V_h^2 + 4/3V_t^2$ . Values of hydrodynamic velocity and 'fast sound' velocity are given for melts.

symmetry, the two transverse branches are degenerate, and in the spectra of monatomic liquids, only two excitation branches should be observed: longitudinal and transverse. The three or four branches in the second Brillouin pseudozone observed in [44–46] are apparently an artifact of the incorrect analysis of the correlation functions of transverse and longitudinal flows.

## 6. Excitation spectra of superfluid and normal liquids: find five differences

As we have seen, research in recent years has enabled detailed studies of many features of the spectra of collective excitations in ordinary liquids and glasses. These spectra can now be compared with those of superfluid helium more carefully.

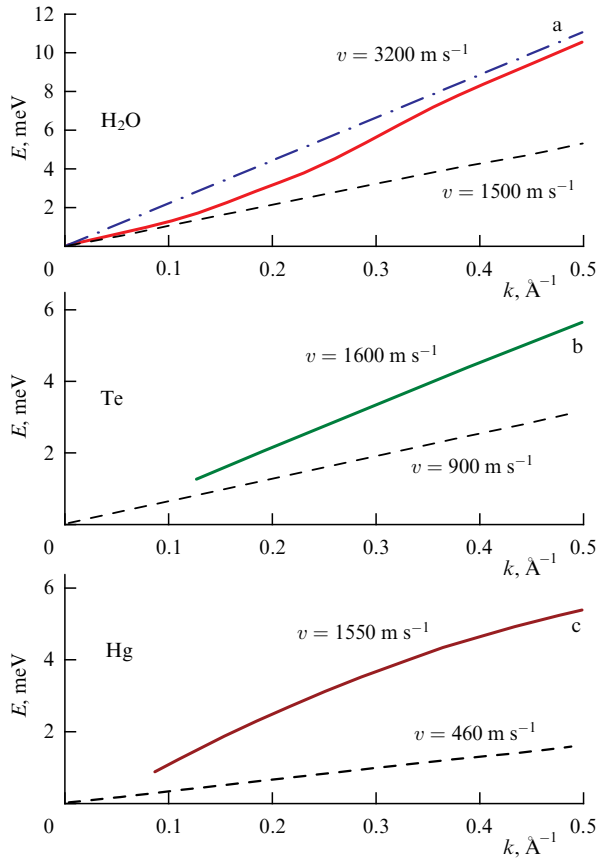


**Figure 12.** ‘Fast sound’ of anomalously large magnitude in (a) water, (b) tellurium melt, and (c) mercury fluid near critical point [38]. Initial parts of longitudinal excitation spectra (solid lines) and lines corresponding to hydrodynamic velocities of sound (dashed lines) are shown.

In addition, the quality of experimental data on superfluid helium has also improved significantly over the past 50 years. It turns out that, in addition to the maximum and minimum, the spectrum also contains a plateau in the range of large wave vectors and the ‘end point’ of the spectrum at approximately  $k = 3.6 \text{ Å}^{-1}$  [8, 47] (Fig. 16).

Note that such a plateau and the ‘end point’ are absent in the spectra of ordinary liquids, where we recall that, as the wave vector increases, the frequency of collective excitations increases without bound, switching to the regime of ballistic motion of individual particles. Interestingly, the plateau and the ‘end point’ were also predicted by Pitaevskii before their reliable experimental detection, and they bear his name [23, 48]. In this regard, it would be fair to say that the contributions of Pitaevskii and Landau to the description of the spectrum of superfluid helium are comparable. We see that the magnitude of the damping of the spectrum is not the only parameter that distinguishes normal and superfluid liquids. Figure 17a shows the excitation spectra of normal and superfluid helium for comparison [8]. The spectrum of normal helium has a shape typical of all inert liquids. We list the main differences between the spectra. First, the excitation spectra are significantly broadened in the normal state of helium. This was expected, but the quantitative comparison is impressive: the damping of excitations in the superfluid state at temperatures  $T < 1 \text{ K}$  is several thousand times less than in the normal state. Moreover, the damping of the spectra in superfluid helium is an order of magnitude less than the

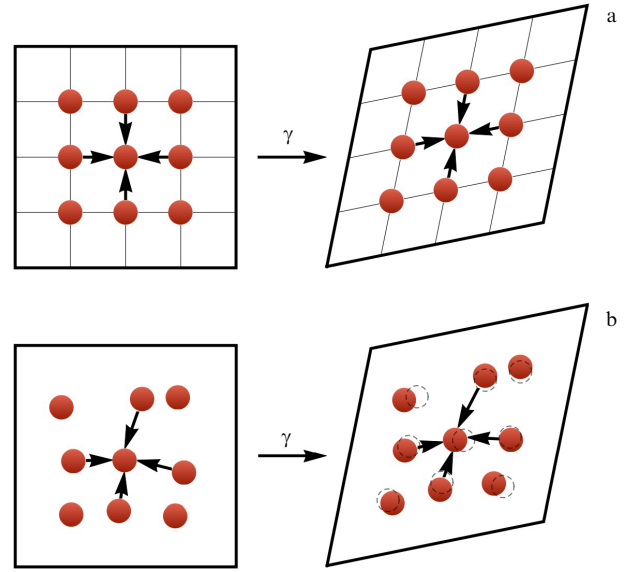


**Figure 13.** Illustration of ‘nonaffinity’ of particle displacements in disordered systems. (a) Shear stresses in a crystal do not lead to uncompensated forces acting on particles inside the region. (b) In a disordered system, shear stresses lead to uncompensated forces and displacement of particles within the nanoregion.

damping of phonons in crystalline helium at the same temperatures. In addition, in normal helium, the damping increases rapidly at large wave vectors, but, in superfluid helium, on the contrary, the spectra are broadened even less in the roton minimum range than in the phonon region of small wave vectors. Such a small damping in superfluid helium spectra is observed in a wide range of pressures up to crystallization [8, 47] (Fig. 17b).

The absence of damping of the superfluid helium spectrum is associated just with its superfluidity and not with low temperatures. To illustrate this, we show the excitation spectrum of He3 at a temperature of 0.12 K [49] (Fig. 17c). It is evident that the damping of the spectrum is practically the same as in He4 in the normal state, although the spectra were obtained at a temperature 20 times lower.

We note that the spectrum width in the superfluid state correlates to a certain extent with the fraction of the ‘normal’ component. We have discussed spectra at temperatures of the order of 1 K and below, where the fraction of the ‘superfluid’ component is almost 100%. At 1.5–2 K, the fraction of the ‘normal’ component in superfluid helium is very large (10 to 50%), and the excitation spectra become significantly broadened [8]. At the same time, no direct correspondence is observed between the fraction of the ‘normal’ component and the broadening. For example, at a temperature of 1.96 K, where the fraction of the ‘normal’ component is approximately 50%, the spectrum broadening is 1.7 K, which is 12 times (and not 2 times, as might be expected) less than the broadening in the normal state (Fig. 18). At a temperature of 1.5 K, where the conventional fraction of the ‘normal’ component is approximately 10%, the spectrum broadening is 0.34 K, which is 60 times (and not 10 times, as might be expected) less than the broadening in the normal state (see Fig. 18). That is, the ‘normal’ component in a superfluid liquid at  $T < 2.17 \text{ K}$  makes an effective contribution to the spectrum broadening six times less than in the normal state at  $T > 2.17 \text{ K}$ . We note that spectrum broadening in the range

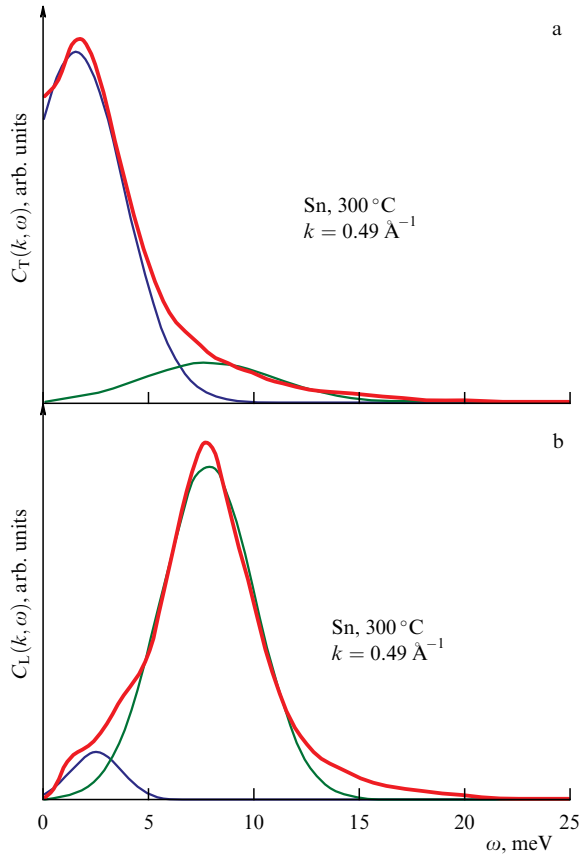


**Figure 14.** Correlation functions of (a) transverse and (b) longitudinal flows for tin atoms according to calculations in [42]. Flows are shown by thick red lines. Mixing of longitudinal and transverse branches is observed: correlation function of transverse flow contains a longitudinal component (smeared peak at high frequencies); correlation function of longitudinal flows contains a transverse component (moderate peak at low frequencies).

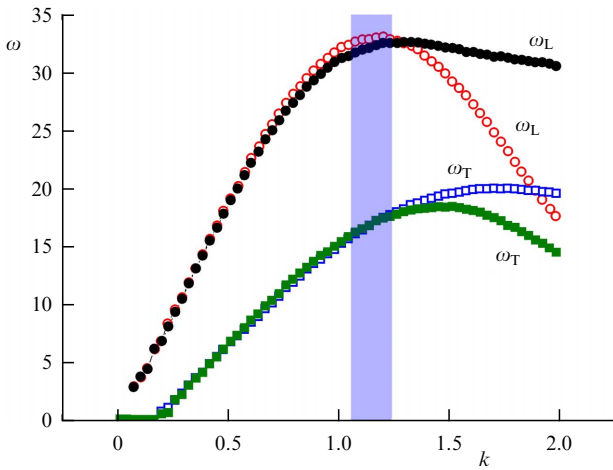


**Figure 15.** Spectra of longitudinal  $\omega_L$  and transverse  $\omega_T$  excitations in a fluid of particles with Lennard-Jones potential according to computer simulation in [43]. Unfilled symbols show ‘wrong’ spectra with false branch intersections obtained by standard method of separate analysis of correlation functions of flows without accounting for their mixing. Solid symbols show correct spectra obtained by joint processing of correlation functions of flows with their mixing taken into account.

of 1–2.2 K was investigated in most studies for wave vectors up to the roton minimum. The broadenings in the range of the maximum ( $k = 1.1 \text{ \AA}^{-1}$ ) and minimum ( $k = 1.95 \text{ \AA}^{-1}$ )

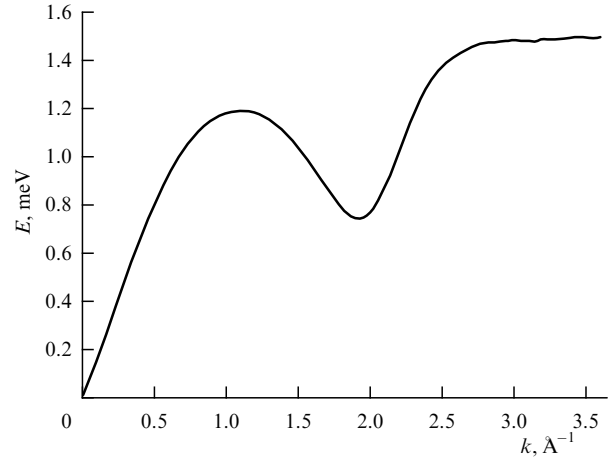


**Figure 16.** Spectrum of collective excitations in superfluid helium at ultralow temperatures  $T < 0.1 \text{ K}$  according to data in [47].

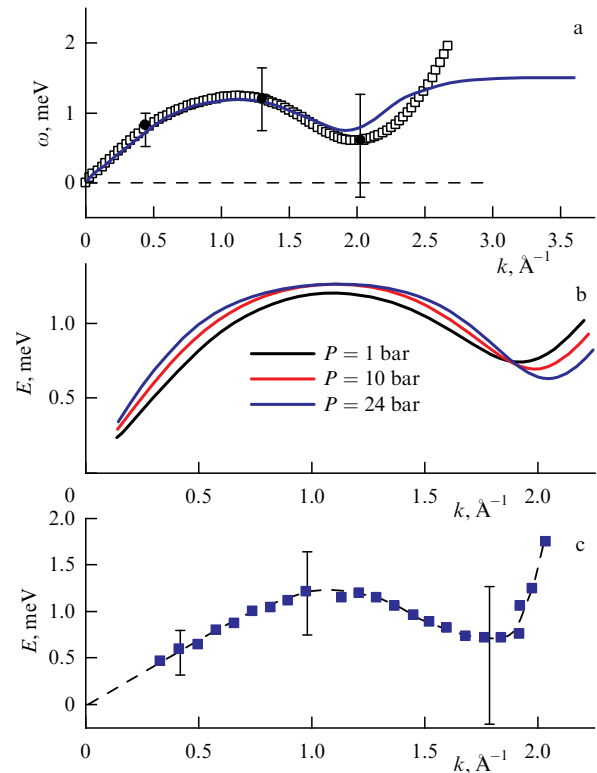


**Figure 17.** (a) Spectrum of collective excitations in superfluid helium 4 at  $T = 0.5 \text{ K}$  (solid blue line) in comparison with excitation spectrum in helium in normal state at  $T = 2.5 \text{ K}$  (squares) [8]. Vertical segments indicate magnitude of effective damping of excitation spectrum in normal state on corresponding wave vectors. Damping in superfluid state does not exceed line thickness. (b) Excitation spectra in superfluid helium 4 at different pressures at  $T = 0.1 \text{ K}$  [47]. Damping does not exceed line thickness. (c) Excitation spectrum in normal state of helium 3 at  $T = 0.12 \text{ K}$  [49]. Vertical segments show magnitude of effective damping of excitations on corresponding wave vectors.

turned out to be close in magnitude (see Fig. 18). At higher wave vectors, from 2 to  $3.5 \text{ \AA}^{-1}$ , the spectra were recorded at 1–2.2 K in only one study [50]. The spectrum itself was constructed in that study at only one temperature, 1.35 K; however, the data on the dynamical structure factors presented there allow hypothesizing that the ‘post-roton’

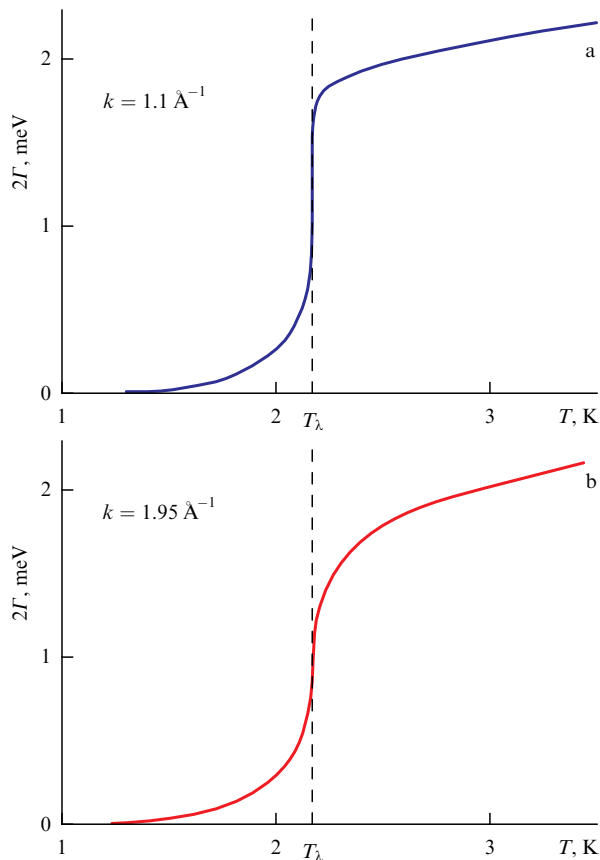


**Figure 18.** Temperature dependence of effective damping of collective excitations in helium [8] for different wave vectors: (a) near maximum of  $\omega(k)$  dependence and (b) near roton minimum. At  $T < 1$  K, damping does not exceed 0.01 K.

part of the spectrum at temperatures of 1.6 K and 1.92 K is a combination of a broadened plateau with moderate damping and a very broadened branch of the spectrum with energies from 2.5 to 4 meV, similar to that part of the spectrum for the ‘normal’ state of helium. It is obvious that additional experimental studies are required for this region of the superfluid helium spectrum in this temperature range.

In the superfluid state, it is not possible to record any traces of transverse excitations. Positive dispersion of sound in superfluid helium is observed, but at a very low level (of the order of 1–2%) [8], which can be naturally explained in the framework of the modern theoretical description of superfluidity in helium. At the same time, recent measurements of spectra at ultralow temperatures ( $< 0.1$  K) [47] have shown that positive dispersion can reach 5% at low pressures and is absent at pressures above 10 bar. Evidently, the issue of dispersion of longitudinal sound waves awaits additional experimental and theoretical studies.

The positions of the maximum and minimum on the  $\omega(k)$  dependences of normal and superfluid helium almost coincide, but, as the wave vector increases further, the dependences strongly diverge, as we have already mentioned. Instead of further blurring of the spectrum and a transition to the regime of ballistic excitation of individual particles, as is the case in ‘normal’ helium, a plateau in the  $\omega(k)$  dependence is observed in the superfluid state, with almost no damping and an abrupt end of the spectrum at  $k = 3.6 \text{ Å}^{-1}$ . As noted above, the vicinity of the  $\omega(k)$  dependence in the region of the

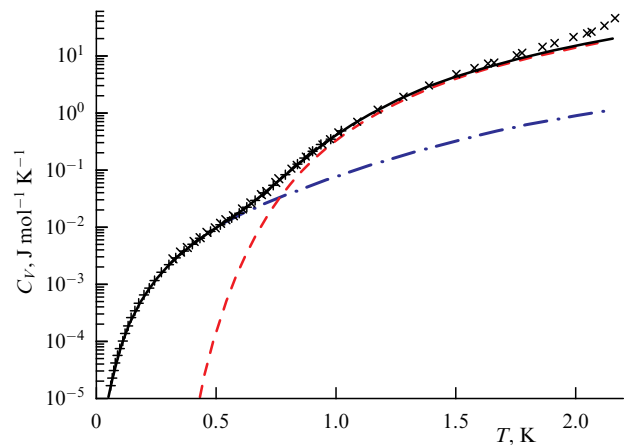


**Figure 19.** Isochoric heat capacity of helium 4 in superfluid state in temperature range of 0.05–2.1 K. Crosses show experimental data. Dashed-dotted and dashed lines are respective theoretically calculated phonon and roton contributions. Solid line is sum of these contributions [47].

minimum for normal helium is not a separate specific excitation, but simply a blurred ‘double’ of excitations at zero wave vectors with a shift by the reciprocal lattice pseudovector. At the same time, the roton part of the spectrum in superfluid helium was proposed by Landau to explain the temperature dependence of the heat capacity of helium. The accuracy of measurements in the 1940s was insufficient for unambiguous conclusions, and it could be assumed that the behavior of the heat capacity is associated with other factors, for example, with the proximity of the  $\lambda$  phase transition point. However, modern data on precision measurements of the heat capacity of helium in the range of 0.05–2 K [47] (Fig. 19) indicate that the roton contribution to the heat capacity of superfluid helium is certainly present. Moreover, at temperatures  $T > 0.7$  K, this contribution is decisive and describes the temperature dependence of the heat capacity up to 1.3 K surprisingly accurately.

Therefore, arguments about Brillouin pseudozones, valid for normal liquids, are not applicable to superfluid helium. That is, all parts of the superfluid helium spectrum at wave vectors  $k$  from 0 to  $3.6 \text{ Å}^{-1}$  are equally real and must be taken into account in analyzing the thermodynamic properties. Roton excitations near the minimum in superfluid helium are not some kind of a smeared ‘double’ of phonons at small wave vectors. Why do the arguments about spectrum blurring and large damping, as well as the concept of Brillouin pseudozones, not work for superfluid helium? It looks as if superfluid helium behaves like a structureless homogeneous continuous medium for all wavelengths and all excitations, which are eigenexcitations and are not damped. At the same time, the time-averaged atomic structure of helium does not change significantly under transition to the superfluid state. In contrast to the radical modification of the dynamical structure factor under transition from the normal to the superfluid state, the static structure factor remains practically unchanged [51] (Fig. 20). We return to this issue in Section 8.

To summarize, we list once again the main differences between the spectra of collective excitations of helium in the ‘normal’ and superfluid states.

(1) The superfluid helium spectrum has anomalously small damping for all wave vectors up to  $k = 3.6 \text{ Å}^{-1}$

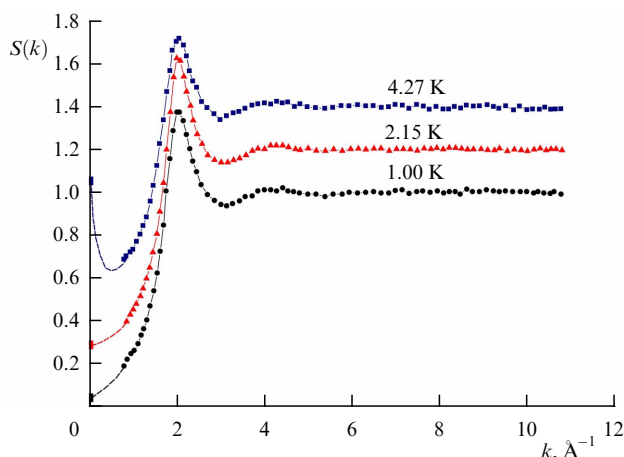


**Figure 20.** Static structure factor of liquid helium 4 obtained by neutron scattering [51]. Data presented are for normal state near boiling point, for superfluid state, and near  $\lambda$ -transition point.

(thousands of times smaller than in the normal state at temperatures below 1 K, and an order of magnitude smaller at temperatures near the  $\lambda$ -point).

(2) No transverse excitations are observed in the superfluid state. The question of ‘fast sound’ remains open: it is observed at low pressures and is absent at pressures above 10 bar.

(3) There are no Brillouin pseudozones or reciprocal lattice pseudovectors in a superfluid liquid. All parts of the spectrum are equally real.

(4) Excitations near the ‘roton’ minimum must be taken into account when analyzing the heat capacity of superfluid helium, in contrast to the normal state of helium and all other liquids (see a more detailed discussion in Section 7).

(5) In the range of large wave vectors  $k > 2.5 \text{ \AA}^{-1}$ , the spectra of superfluid and normal helium are radically different. Instead of a smooth crossover to the ballistic regime spectrum of single-particle excitations, which occurs for normal liquids, a flat plateau and the point of an abrupt end of the spectrum are observed in the superfluid helium spectrum.

Despite the significant differences between the spectra of normal and superfluid helium, their genetic relation is obvious: the spectra smoothly transform into each other, and the positions of the maximum and minimum in the spectrum remain almost unchanged. This fact, as well as the almost complete similarity of the static structure factors, must be taken into account when constructing a theory of superfluidity.

## 7. Collective excitations and heat capacity of normal and superfluid liquids

As noted in Section 2, the density of states of collective excitations determines the thermodynamic properties of substances, including important characteristics such as heat capacity. For crystals, this has been well known for over 100 years, starting with Einstein’s and Debye’s heat capacity models for solids. Quasiphonon spectra of collective excitations in liquids and glasses started being considered only in recent decades [9, 11]. Previously, models describing the heat capacity of liquids were virtually absent, and information on the pair correlation function of the particle distribution and

the effective potential of interparticle interaction was used to calculate the heat capacity [52]. The pair correlation function, in turn, is usually taken from experiment or from computer modeling data. We have shown that the temperature dependence of the heat capacity of liquids can be described well within the quasiphonon approach. For almost all substances, the melting point exceeds the Debye temperature. The exceptions are helium 3, helium 4, and hydrogen, whose melting and boiling points are significantly lower than the Debye temperature due to the large contribution of zero-point oscillations of particles. For such liquids in the normal state, A.F. Andreev proposed the term ‘semiquantum liquids,’ in contrast to purely quantum Bose and Fermi liquids (helium 4 and helium 3) in the superfluid state. We return to these substances later. For most crystals, the isochoric heat capacity near melting is  $C = 3k_B$  per particle (where  $k_B$  is the Boltzmann constant) or  $3R$  per mole (the Dulong–Petit law). The heat capacity of melts of these substances near the melting point is also close to  $3k_B$  per particle, which is explained by the presence of both longitudinal and transverse excitations in almost the entire frequency range. As noted above, the spectrum of shear waves of liquids has a wave-vector gap (the  $K$ -gap), whose magnitude increases with temperature. This means that shear excitations ‘depart’ from the spectrum of liquids under heating, which results in a decrease in heat capacity from  $3k_B$  to  $2k_B$  per particle on the Frenkel line [11, 53]. The ‘departure’ of excitations from the spectrum corresponds to an increase in the concentration of particles moving ballistically. Initially, in glass or a viscous liquid of  $N$  particles, there are  $3N$  oscillatory modes:  $N$  longitudinal and  $2N$  transverse. Each excited mode stores the energy  $k_B T$  (where  $1/2k_B T$  comes from the kinetic and potential parts of the energy). The ‘departure’ of a mode from the spectrum means the disappearance of the potential part of the energy of a given mode. The ‘departure’ of three modes from the spectrum is equivalent to the appearance of one free particle. Accordingly, the ‘departure’ of  $2N$  modes means that, on average,  $2/3$  of the particles in the liquid move ballistically, i.e., are in the ‘gaseous’ component of the density of states (Fig. 2c). Within the quasiphonon approach, a further decrease in the heat capacity of fluids under heating at supercritical pressures, from  $2k_B$  to  $1.5k_B$ , is associated with the ‘departure’ of longitudinal excitations from the spectrum, starting with short-wavelength ones [9, 11]. The gap in the spectrum of shear excitations can be associated with the threshold frequency  $\omega_F$  (Frenkel frequency) [9, 11, 53]. Then, within the Debye model (with a quadratic density of states depending on the energy and a limit Debye frequency  $\omega_D$ ), the energy of the liquid per particle is

$$E = k_B T \left[ 3 - \left( \frac{\omega_F}{\omega_D} \right)^3 \right].$$

This simple formula predicts the temperature dependence of the heat capacity fairly well (Fig. 21).

However, more accurate modeling data show that the heat capacity decreases almost linearly, depending on the gap magnitude in terms of the wave vector [54] (Fig. 22). This means that the density of states of shear excitations is not Debye, but is almost constant in a wide energy range. We note, however, that, in the limit of small wave vectors, a linear dispersion law and small damping must necessarily lead to a quadratic (Debye) density of states. Deviation from a



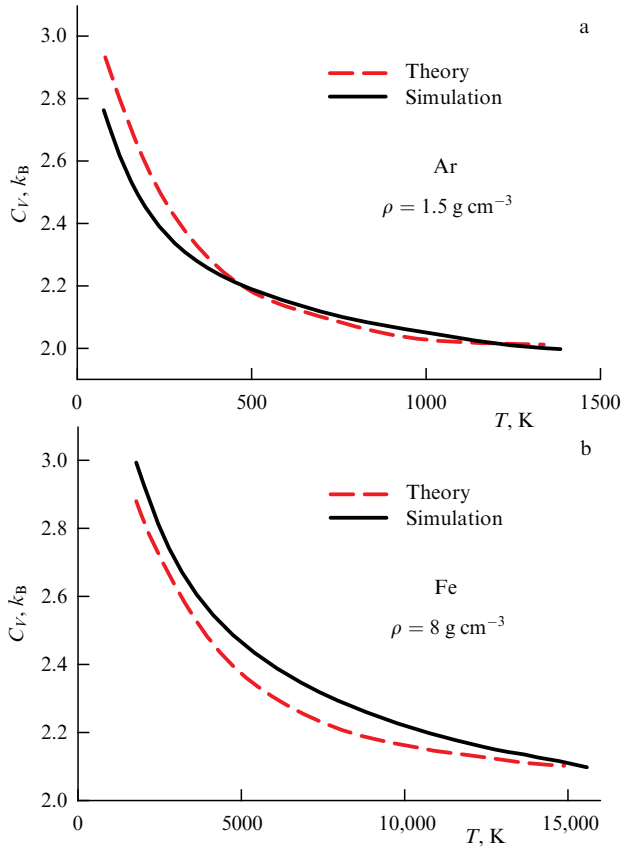


**Figure 21.** Temperature dependence of heat capacity per particle on isochores for (a) argon fluid (Lennard-Jones potential) and (b) iron melt. Solid lines: computer simulation data, dashed lines: calculation within simplified Debye model [53].

quadratic dependence for the density of states in a liquid occurs only starting from a certain value of the wave vector.

Let us now consider the behavior of the heat capacity of liquids and its connection with the excitation spectra in the low-temperature range. It turns out that, at low temperatures, helium 4 and hydrogen demonstrate an almost linear increase in the heat capacity with temperature [55] (Fig. 23). At normal pressure, the temperature interval between melting and boiling for both liquids is small, but at pressures much higher than critical, a quasilinear increase in heat capacity with temperature is observed over a sufficiently wide temperature interval. Previously, there were attempts to explain this behavior by analogy with the linear behavior of the low-temperature heat capacity for glasses [56]. In many glasses, at temperatures much lower than the Debye temperatures, a linear dependence of heat capacity with temperature is observed, which has been explained within the model of excitations of the two-level systems.

Recall that the phonon heat capacity at low temperatures is proportional in the Debye model to the temperature cubed,  $C \sim T^3$ , which is satisfied well for most crystals. The same dependence gives a good quantitative description of the heat capacity of superfluid helium at temperatures below 0.5 K. We discuss the heat capacity of the superfluid state of helium 4 and helium 3 below. However, in the Debye model, the heat capacity actually has a cubic dependence on temperature only at temperatures significantly below  $0.1\theta_D$ , where  $\theta_D$  is the Debye temperature. Above  $0.1\theta_D$ , the temperature dependence of the heat capacity deviates strongly from the cubic

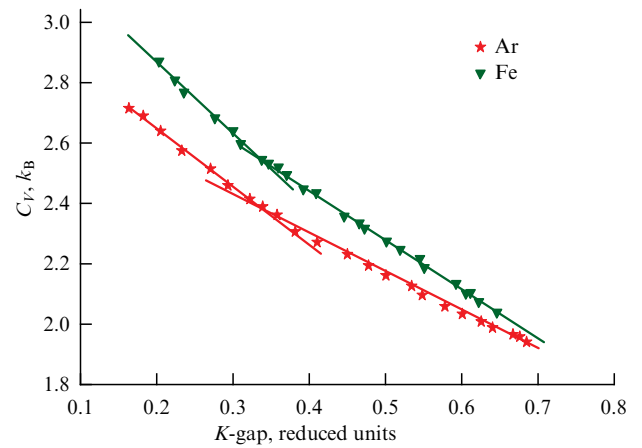


**Figure 22.** Dependence of heat capacity on wave-vector gap (K-gap) for transverse excitations for argon and iron fluids according to data in [54].

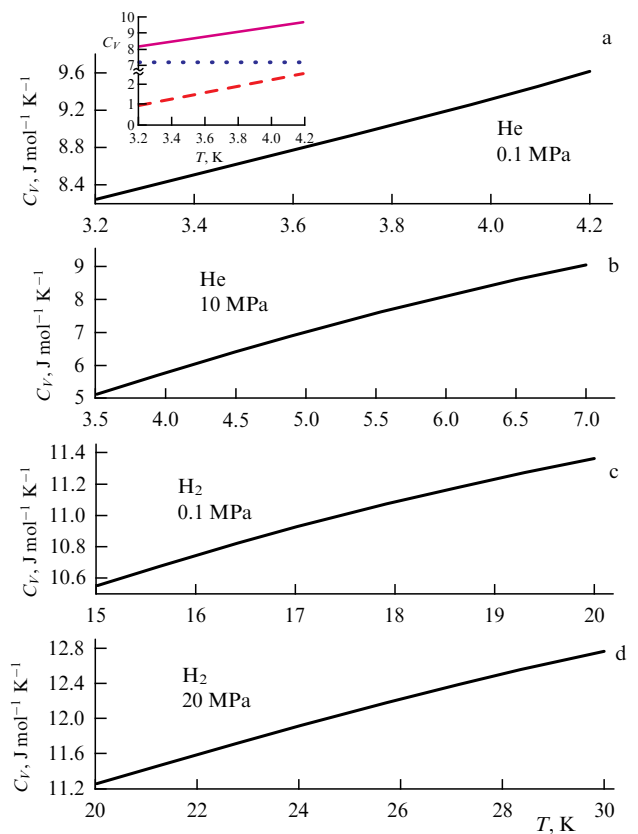


**Figure 23.** Temperature dependence of heat capacity at different pressures for (a, b) liquid helium and (c, d) hydrogen. Inset shows conventional contributions to heat capacity of liquid helium: dashed line is Debye contribution (40% of atoms), dotted line is temperature-independent quasigaseous contribution (60% of atoms).

dependence and approaches a linear one. Indeed, at  $T \approx 0.16\theta_D$  (more precisely,  $0.164\theta_D$ ), the temperature dependence of the heat capacity in the Debye approximation exhibits an inflection (the second derivative vanishes). Therefore, in the range of  $0.12\theta_D$ – $0.2\theta_D$ , the dependence is very close to linear. For example, for diamond, where room temperature is approximately 15% of the Debye temperature, a virtually linear dependence of the heat capacity on temperature is indeed observed in the range 250–350 K. It was

in the range of  $0.12\theta_D$ – $0.2\theta_D$  that the measurements for helium and hydrogen presented in Fig. 23 were carried out ( $\theta_D \approx 26$  K for helium and  $\theta_D \approx 120$  K for hydrogen). Thus, at first glance, the almost linear dependence of the heat capacity of helium and hydrogen can be explained trivially by taking phonons into account in the Debye approximation. But no quantitative correspondence is then observed: the experimental heat capacity values are significantly higher than the calculated ones, and the increase in heat capacity with temperature is lower than the calculated one. According to the Debye formula, the heat capacity at respective temperatures of  $0.1\theta_D$ ,  $0.15\theta_D$ , and  $0.2\theta_D$  is approximately 2, 5, and  $9 \text{ J mol}^{-1} \text{ K}^{-1}$ . Obviously, there is an additional significant contribution of excitations of a certain type to the heat capacity. As we have noted, the roton contribution in the normal state of the liquid cannot exist, because these are ‘fake’ excitations relating to the second and third pseudo-Brillouin zones. Moreover, if the roton contribution to the heat capacity of superfluid helium [47] is formally extrapolated above the  $\lambda$ -point, then we obtain unphysically large values from  $25 \text{ J mol}^{-1}$  at 2.2 K to  $100 \text{ J mol}^{-1}$  at 4.2 K. It is logical to assume that an additional contribution to the heat capacity of normal liquid helium and liquid hydrogen is due to single-particle excitations that are hops of particles in the liquid. In the density of states, this contribution corresponds to the imaginary frequencies in Fig. 2b or the ‘gaseous’ component in Fig. 2c. The contribution to the heat capacity from such particles is  $(3/2)k_B$  per particle. In most liquids near the melting point, the fraction of particles that have ‘departed’ from the vibrational spectrum of collective excitations is small on average, amounting to 10 to 20%. But in helium and hydrogen, this fraction is apparently much higher, because these fluids have very low viscosity, and the temperature ranges under consideration are close to their critical points. If we assume that the fraction of hopping particles is 50 to 60%, then the corresponding constant contribution to the heat capacity is  $6$ – $8 \text{ J mol}^{-1} \text{ K}^{-1}$ . Taking into account that the temperature-dependent Debye phonon contribution decreases by a factor of 2–2.5 (only 40 to 50% of particles participate in the formation of the quasiphonon spectrum), the sum of the two contributions to the heat capacity is in excellent agreement with all experimental data. Thus, hydrogen and helium at below-boiling temperatures are close to the corresponding Frenkel lines (recall that the Frenkel line corresponds to approximately 67% of particles in the quasigaseous phase), and their heat capacity is 70 to 90% determined by the contribution from particle hops, which depends weakly on temperature, and 10 to 30% is determined by the temperature-dependent quasilinear Debye ‘phonon’ contribution (see the inset in Fig. 23a). At high pressures (10 MPa), the total heat capacity of helium is 75% the Debye contribution and 25% the hopping contribution.

We now consider the behavior of the heat capacity of helium 3. In contrast to helium 4 and hydrogen, the temperature range of the existence of the liquid phase of helium 3 in the normal state is very large on a logarithmic scale: the temperature changes by three orders of magnitude. This is due to the very low temperature of the transition to the superfluid state,  $T \approx 2$  mK. The temperature dependence of the heat capacity of helium 3 in the normal state consists of several quasilinear parts (Fig. 24).

The behavior of helium 3 is more complex, because the He3 atomic nuclei have spins and are Fermi particles. The heat capacity of a degenerate gas of Fermi particles (or an

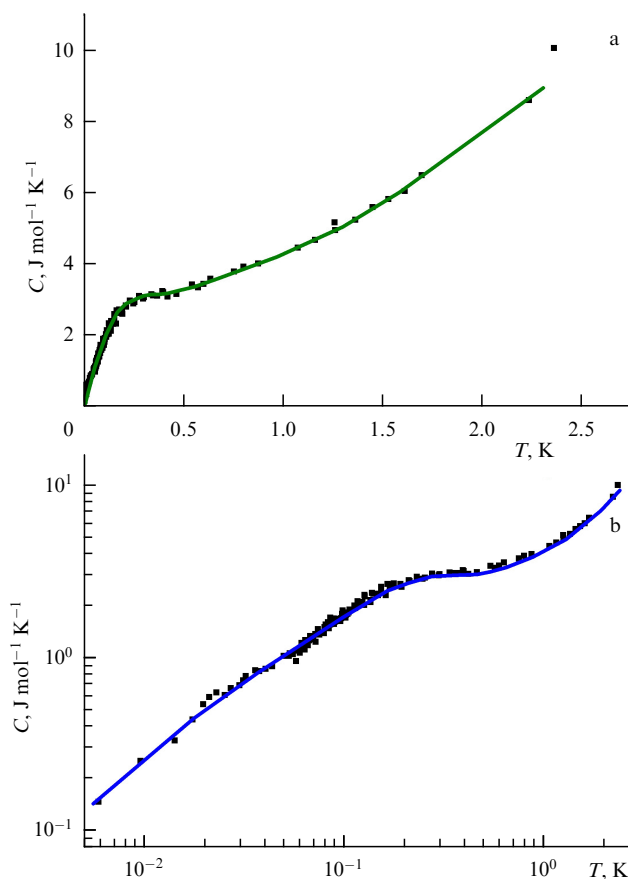


**Figure 24.** (a) Heat capacity of helium 3 in normal state according to data in [57, 58]; (b) same data on double logarithmic scale.

ideal Fermi liquid) has a linear dependence on temperature, and the leading contribution to the heat capacity for He3, especially at ultralow temperatures, is associated with the behavior of the magnetic moments of atoms [57]. At the same time, there are additional contributions, linear and cubic in temperature, in the range of 0.5 to 2.5 K [58]. The data presented in Fig. 24 allow hypothesizing that part of the heat capacity is associated with both the Debye ‘phonon’ contribution and the contribution from particle hops. The latter contribution depends more strongly on temperature than for He4, possibly because the temperatures are much lower for He3.

We now consider the behavior of the heat capacity of helium isotopes in the superfluid state. When discussing Fig. 19 in Section 6, we already mentioned that, in a wide temperature range from 0.05 to 1.3 K, the experimental heat capacity of superfluid helium 4 is perfectly described as the sum of the phonon contribution (cubic in temperature) and the roton contribution (exponential in the inverse temperature) [8, 47]. At temperatures above 1.3 K, the experimental data are observed to slightly deviate from the calculated ones towards higher heat capacity values. The deviations become significant at temperatures above 1.8 K. Such deviations are usually associated with a certain part of the normal fraction appearing at these temperatures, and the spectra, including the main roton part, are broadened at these temperatures [8] (see Section 6). However, this should at first glance lead to a decrease in the roton contribution, whereas the experimental data demonstrate an additional increase in the heat capacity. Atoms in the ‘normal’ state can make a quasigaseous



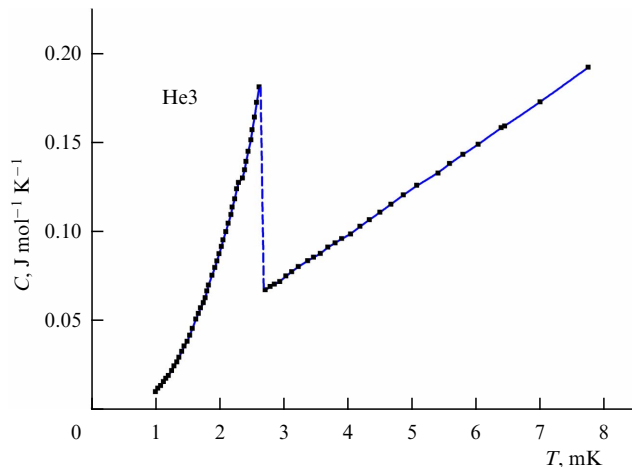


**Figure 25.** Heat capacity of helium 3 in vicinity of transition to superfluid state at increased pressure according to data in [59].

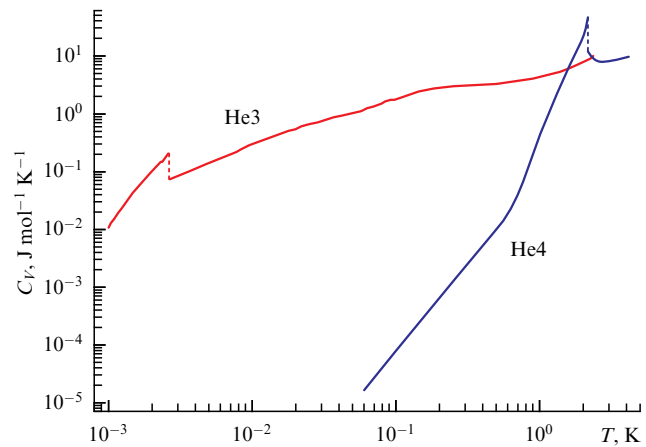


**Figure 26.** Heat capacities of helium 4 and helium 3 in entire temperature range, including regions of superfluid and normal states, according to data in [55, 57–59].

contribution (as they do above the transition temperature). It can also be hypothesized that small deviations of the experimental data from the theoretical dependences are associated with a weak and difficult-to-register temperature dependence of the energy of the roton minimum [8]. It is also possible that the discrepancy between the experimental and calculated data is associated with the fluctuation influence of the  $\lambda$ -transition at 2.17 K. The heat capacity of superfluid helium 3 has been investigated in fewer studies and with less accuracy, due to the complexity of studies at such low temperatures. The temperature dependence of the heat capacity is close to the ‘phonon’ cubic one (Fig. 25). We note that the temperature of the transition to the superfluid state for helium 3 increases from 2 to 2.6 mK as pressure increases [59]. This fundamentally distinguishes helium 3 from helium 4, where the  $\lambda$ -transition temperature decreases with pressure [8]. It is no coincidence that the superfluidity of helium 3 was first discovered at increased pressures. In addition, in contrast to helium 4, the  $P, T$  phase diagram of superfluid helium 3 contains two phases with different characteristics, A and B. A discussion of these details, however, is beyond the scope of this review.

There are no reliable experimental data on the spectra of collective excitations in the superfluid state of helium 3. Nevertheless, the similarity of these spectra in the normal state [60] leaves no doubt that the spectra of the two isotopes are almost identical in the superfluid state (taking the renormalization of energies due to the difference in masses and interaction potentials into account). Roton excitations in helium 3 cannot exist at such low temperatures, and only the phonon contribution remains. Above the temperature of the transition to the superfluid state, a linear dependence of the heat capacity on temperature is observed, corresponding to the behavior of an ideal Fermi liquid with Fermi particle masses equal to approximately three times the mass of atoms [59]. In Fig. 26, for completeness, we present data on the heat capacity of both helium isotopes over the entire temperature range, including the superfluid and normal states. Note the huge difference among the heat capacities of the helium isotopes at ultralow temperatures. It amounts to five orders of magnitude at 0.05 K and is estimated at 8 to 10 orders of magnitude at temperatures of 2 mK and below.

A comparison of the properties of helium isotopes is beyond the scope of this review. Such comparisons have

been made in many papers, for example, in a recent note in *Physics–Uspekhi* [61], helium isotopes were compared in detail as regards the melting thermodynamics. We nevertheless discuss several key points that are important in the context of this paper. In the classical limit, isotopic effects in condensed matter are observed only for those quantities that directly include particle masses, such as density, oscillation frequency, and speed of sound. Thermodynamic properties of different isotopes coincide, because the particle mass does not affect the interparticle interaction in the classical limit. Quantum isotopic effects are associated with zero-point oscillations and zero-point energy, which differ for different isotopes. As a rule, such effects are very small. For example, for the C12 and C13 diamond isotopes, the difference in mass is 8%, and the difference in the vibration frequencies of carbon atoms in the classical limit is 4%. Diamond has a record-high Debye temperature of  $\approx 2000$  K, and hence diamond is a ‘quantum’ crystal at room temperature. However, quantum isotope effects are only 0.2% for optical vibration frequencies, and 0.1% for the lattice constant [62]. This is due to the very strong covalent interaction between diamond atoms, which changes only slightly when taking the zero-point energy into account. The same picture is observed in isotopes of other substances. The contribution of the zero-point energy of vibrations only slightly modifies the effective constants of interparticle interaction, weakening the constants to a greater extent for a lighter isotope due to the larger amplitude of vibrations. Helium isotopes are unique objects in this sense, for which quantum isotope effects are gigantic. This is due to both the high values of the Debye temperatures compared to the temperatures of the critical points and the very weak van der Waals interparticle interaction. As a result, the densities of helium isotopes in the liquid state differ by 1.8–2 times, although the particle masses differ by ‘only’ 33%. This means a radical weakening of the effective interaction constants in helium 3 compared to helium 4. The speed of sound in liquid helium 3 is 10–20% less than in helium 4 [63]. Accordingly, the bulk compression moduli of the isotopes differ by more than 2.5 times, and the effective interaction constant, by 60 to 80%. Weaker interparticle interaction in helium 3 leads to a lower boiling point (the critical point temperatures differ by 60%). Thus, isotopic effects in helium for the parameters of interparticle interaction significantly exceed the actual ratio of the isotope

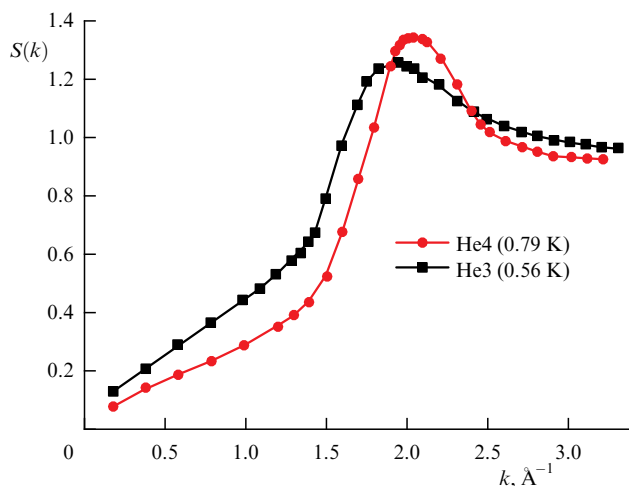


**Figure 27.** Comparison of static structure factors of helium 3 and helium 4 [64].

masses. This means that the spectra of collective excitations in helium isotopes should differ. The hypothesis of their complete similarity made in [60] is not entirely correct and was made without taking the large measurement error and large damping into account. A smaller average interparticle distance in helium 4 compared to helium 3 should lead to higher values of the wave vector corresponding to the maximum on the dispersion curve  $\omega(k)$ . Indeed, the position of the main maximum of the static structure factor for the two isotopes differs by approximately 12% [64] (Fig. 27).

Consequently, the positions of the maxima of the dispersion curves  $\omega(k)$  (the boundaries of the first Brillouin pseudozone) must also differ. A smaller value of the speed of sound in helium 3 than in helium 4 means a decrease of 10 to 20% in the slope of the dispersion  $\omega(k)$  on the linear part and a decrease of 20 to 30% in the frequency at the maximum of the curve. It is clear that, for helium 3, further studies are required to more reliably reconstruct the ‘average’ line of the spectrum dispersion curve  $\omega(k)$ .

To conclude this section, we consider the question posed in Section 2 about the behavior of the entropy of liquids at low temperatures. If a liquid is a thermodynamically equilibrium state down to zero temperature, then, according to the third law of thermodynamics, its entropy must decrease to zero. Of course, proving the third law (Nernst’s theorem) by considering possible quantum states is not very constructive, because a macroscopic system enters a single quantum state at unattainably low temperatures. Therefore, the third law is rather a general empirical rule. Zero entropy corresponds to a single equilibrium (quantum) state. Does this mean that such a liquid must pass into a superfluid state? Besides helium isotopes, a hypothetical equilibrium state of liquid metallic atomic hydrogen at megabar pressures is also considered, and the possibility of superfluidity and superconductivity of such a state is discussed [65]. Zero or very low entropy means a small number of states in the phase space, i.e., the presence of a correlation in the positions of particles and their momenta. Crystals at ultralow temperatures are at first glance a trivial example of such systems. However, even at arbitrarily low temperatures, there are zero-point oscillations in crystals, and, for crystals of light atoms, the amplitude of zero-point oscillations is quite significant. Does it make sense to talk about the correlation of such oscillations? To a certain extent,

it is possible, although the very concept of atomic oscillations is semiclassical. In reality, a more constructive idea is the ‘smearing’ of the positions of crystal atoms over a certain area (of the order of the de Broglie wavelength). In quantum liquids at ultralow temperatures, the effective scale of the ‘smearing’ of particle positions exceeds the interparticle distance, which leads to the indistinguishability of particles and the corresponding quantum statistics. We discuss this issue in more detail in Section 8. Quantum correlations between particles do not necessarily give rise to superfluidity, just as ultralow temperatures of metals do not necessarily give rise to superconductivity. Thus, within the Bardeen–Cooper–Schrieffer mechanism, if the Coulomb interaction parameter is greater than the electron–phonon coupling constant, then superconductivity does not emerge at any temperature. It is possible that, in quantum liquids, there may also be a type of interparticle interaction that prevents the occurrence of superfluidity. We also note that the superfluid state in both helium isotopes occurs at finite and quite large values of entropy.

## 8. Helium excitation spectrum as a key to microscopic description of superfluidity

There is no rigorous theory of helium 4 superfluidity [66]. First of all, it has not yet been possible to theoretically obtain the correct shape of the excitation spectrum. The initial part of the spectrum up to the roton minimum can be obtained either within semiempirical models or more rigorously for a weakly nonideal Bose gas [67, 68]. Even first-principle modeling using path integrals [69] reproduces the spectra barely satisfactorily. First, the post-roton plateau is not reproduced at large wave vectors; second, the effective damping of spectra in the superfluid phase is several times less (rather than thousands of times less) than in the normal phase, as observed in experiment (Fig. 28).

In a number of studies [47, 70, 71], the agreement between theoretical and experimental spectra looks more satisfactory, but the theoretical description again involves empirical parameters in the equations. It is obvious that a correct microscopic description of superfluidity should at least explain all five differences in the spectra of the normal and superfluid phases listed in Section 6. So far, this has not been done in any theoretical work. The concept of the emergence of a Bose–Einstein condensate fraction in superfluid helium is

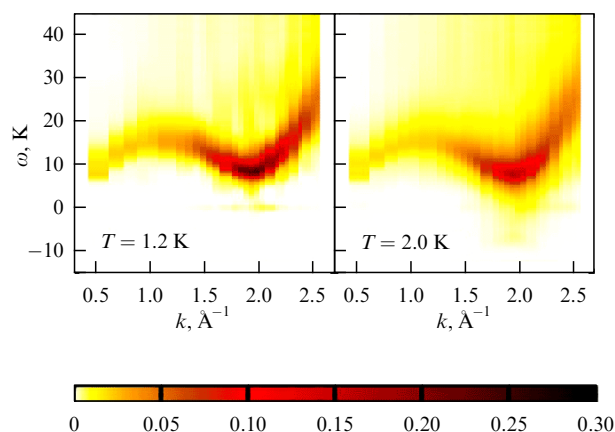


**Figure 28.** Theoretically calculated excitation spectra of helium 4 at two temperatures according to data in [69].

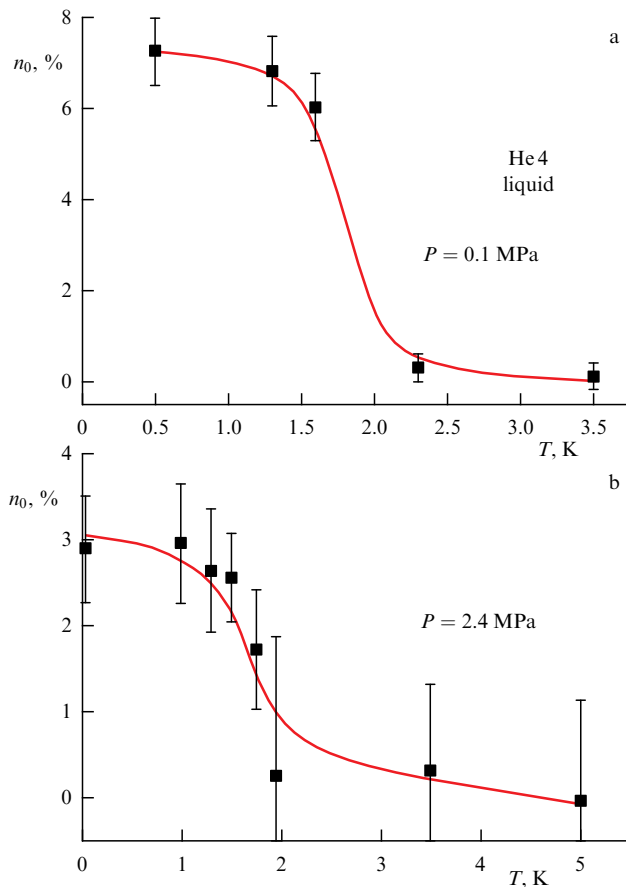


**Figure 29.** Fraction of helium atoms in Bose condensate with zero momentum, estimated from experimental data on dynamical structure factor [8] (a) at normal pressure and (b) at 2.4 MPa.

also very controversial (see [72] and references therein). F. London was the first to suggest a connection between helium superfluidity and Bose–Einstein condensation [73]. Bogoliubov was the first to develop the condensate theory in application to a weakly nonideal Bose gas [74]. Subsequently, numerous attempts were made to theoretically describe the Bose–Einstein condensation in strongly coupled particle systems (see [8] and references therein), but the situation is still far from satisfactory. In the framework of various models, attempts have been made to estimate the fraction of the condensate with zero momentum on the basis of experimental data on the dynamical structure factor [8]. This fraction turned out to be unexpectedly small: 5–6% at 1 K and 7–8% at temperatures close to zero [8]. A natural question arises: how does such a small fraction of atoms ensure the presence of almost the entire superfluid component and all the features of the excitation spectra? Even more so, it turns out that, at increased pressures of about 20 bar, the fraction of atoms in the condensate is even smaller: only 2 to 3% at the lowest temperatures [8] (Fig. 29). At the same time, all the features of the excitation spectra remain exactly the same as at low pressures. It is not very clear how 2% of atoms can determine the properties of the entire system. There are attempts to relate the fraction of atoms in the condensate to the fraction of the superfluid component, but the corresponding expressions contain several empirical parameters. In a number of papers, the existence of a Bose condensate with zero momentum of atoms in helium is generally questioned (see [72] and references therein).

In fact, the two-fluid model of normal and superfluid components is also purely phenomenological. It does describe the temperature dependence of helium viscosity quite well but says nothing about the microscopic mechanisms of the processes [21, 23].

The record-low damping of the spectrum of collective excitations in superfluid helium must mean that they are eigenexcitations. In ordinary liquids and glasses, phonons are eigenexcitations only in the long-wave limit, when the atomic or molecular structure of the liquid ‘is not seen’ and the approximation of a continuous medium is applicable. It is logical to assume that, in superfluid helium, excitations ‘see’ the liquid as a continuous medium. Moreover, this must be so in the entire range of wave vectors. If excitations do not ‘see’ the atomic structure of helium, then the concepts of Brillouin pseudozones and reciprocal lattice pseudovectors must become invalid, which is actually the case. At the same time, the shape of the static structure factor of superfluid helium (see Fig. 20) indicates that, on average, the structure of the liquid remains the same as in the normal nonsuperfluid state. Therefore, **for excitations to ‘see’ liquid helium as a continuous structureless medium on all scales, the short-range order in the liquid must flicker with a frequency higher than the corresponding excitation frequencies.** This does not happen in ordinary liquids, because the particle hopping frequency is always much lower than the frequency of short-wave longitudinal excitations. In helium, the situation is different, because the zero-point energy of particles is higher than the temperature and the excitation energies. Within the Debye model, the zero-point energy is equal to  $(9/8)\theta_D$  [16], which is approximately 30 K for helium. Direct measurements of the kinetic energy of particles actually give values of the order of 14–15 K down to the lowest temperatures [72] (Fig. 30). It can be assumed that the potential component of the zero-point energy is approximately the same in magnitude. This kinetic energy exceeds the excitation energy. The velocity of helium atoms corresponding to the above zero-point kinetic energy is approximately  $250 \text{ m s}^{-1}$ , which is 10 to 20% higher than the speed of sound in helium. The momentum  $P$  of atoms at such kinetic energy corresponds to the de Broglie wavelength of approximately 4 Å, which is slightly greater than the average interparticle distance, and therefore the vibrational and hopping modes are practically indistinguishable. Thus, due

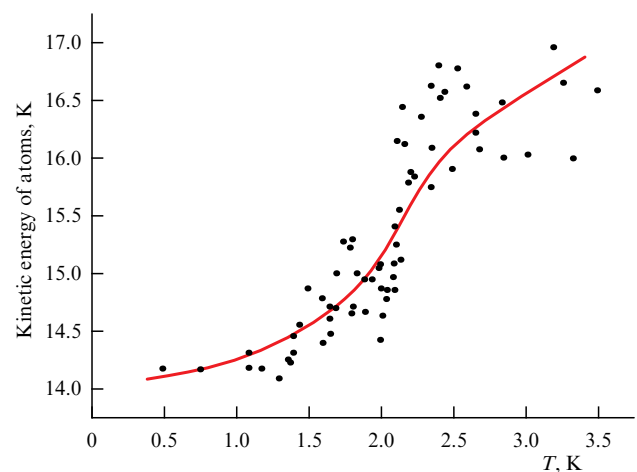


**Figure 30.** Kinetic energy of helium atoms in superfluid and normal states depending on temperature. Data are collected in [72]. Line is roughly drawn for convenience.

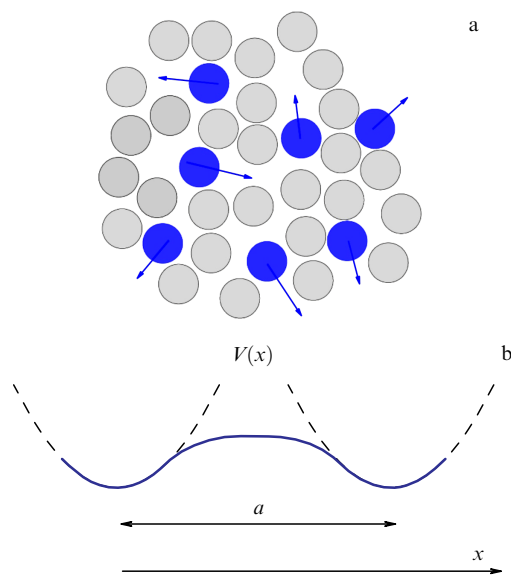


**Figure 31.** (a) Qualitative illustration of hops of mobile helium atoms and (b) corresponding part of potential relief according to data in [72].

to the zero-point energy, helium atoms experience frequent hops all the way down to zero temperature, swapping places. The frequency of these hops exceeds the excitation frequency in the spectrum. We note that the uncertainty of the coordinate for such a zero-point momentum of helium atoms is  $0.3 \text{ \AA}$ , i.e., less than the de Broglie wavelength by  $4\pi$  times. Indeed, for the de Broglie wavelength, we have  $L = h/P = 2\pi\hbar/P$ , while from the Heisenberg relation we have  $\Delta X \geq \hbar/2\Delta P$ . The wave vector corresponding to the momentum of helium atoms at zero temperature is  $1.65 \text{ \AA}^{-1}$ , which is 1.6 times greater than the maximum wave vector for quasiphonon excitations in normal helium at the boundary of the first Brillouin pseudozone.

A possible connection between the constant hops of helium atoms with zero-point energy and superfluidity was recently discussed in [72] (Fig. 31). The author of that article even proposed a new term, ‘Bose sphere,’ by analogy with the Fermi sphere. This means that Bose particles are not in a state with zero momentum, as in a classical Bose condensate, but in a state with a finite momentum corresponding to zero-point energy.

However, such hops, causing flickering of the structure, also occur above the  $\lambda$ -point. It is obvious that, as the temperature decreases, such hops should be increasingly correlated. As was noted in [75], for helium atoms to become indistinguishable in a single quantum state, they must physically swap places (Fig. 32). It can be assumed that the degree of correlation of ‘flickering’ hops of the structure corresponds to the fraction of atoms in the superfluid phase. In this case, the atoms have a single wave function, but by no means the one that corresponds to a condensate with zero-point energy.

Thus, continuous correlated flickering of the short-range order structure in superfluid helium provides a possible explanation, in layman’s terms, of the features of the excitation spectrum in the superfluid state considered in Section 6. The waves ‘see’ the rapidly flickering structure as a continuous structureless medium, and harmonic plane waves are eigenexcitations. In this case, on average, a short-range order structure remains the same as in the normal state,

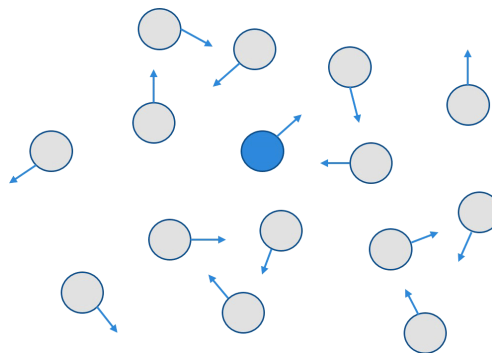


**Figure 32.** Qualitative illustration of correlated hops of helium atoms in superfluid state where atoms swap places.

because the effective smearing of the position of each atom is of the order of  $0.3 \text{ \AA}$ , and the average interparticle distance exceeds  $3 \text{ \AA}$ . The flickering frequency inside each cell significantly exceeds the maximum possible frequency of shear excitations, and therefore transverse collective excitations are absent in the spectra. All features of the collective excitation spectrum are inherited from the normal state, and hence rotons become ‘real’ excitations. The postroton plateau in the excitation spectrum of superfluid helium corresponds to excitations that have an infinite effective mass. This may be due to excitations of a correlated group of a macroscopic number of atoms in the superfluid state. Recall that zero-point energy flickering is the ground (lowest-lying) quantum state of the system. Therefore, such ‘zero-point flickering’ does not manifest itself in any way in the experimental spectra of collective excitations: the excitation spectra are superimposed on the ground state. Moreover, correlated hops of atoms in the ground state correspond to a certain energy level, and are in some sense monochromatic in frequency.

Because of the high zero-point kinetic energy for helium atoms, we must be more diligent in using the concept of a de Broglie thermal wave, where the momentum of atoms is simply assumed to be the thermal momentum  $P_T = (3k_B T M)^{1/2}$ . The magnitude of this momentum tends to zero as the temperature decreases, and the corresponding thermal de Broglie wavelength tends to infinity. Normalization to the thermal de Broglie wavelength allows a comparative analysis of the melting of helium 4 and helium 3 to be successfully performed in the range of intermediate temperatures of the order of the Debye temperatures [61]. But, at ultralow temperatures, due to the zero-point energy, the de Broglie momentum and wavelength in any condensed medium always remain finite. The difference between a condensed medium and rarefied gases is very significant in this context. As noted above, the zero-point energy in condensed media is related to the Heisenberg uncertainty principle. Condensed medium particles (atoms or molecules) are surrounded by neighbors (Fig. 33a), and therefore the uncertainty of the position of each particle cannot be arbitrarily large. In other words, each particle of a condensed medium is in a three-dimensional potential well. The solution of the quantum mechanical problem of the particle behavior in such a well yields a set of energy levels, with the lowest level (the ground state) at a nonzero positive energy. This is the zero-point energy of the particle (Fig. 33b). In the limit of a sufficiently weak interparticle interaction, the particle wave vector associated with the zero-point energy is determined by



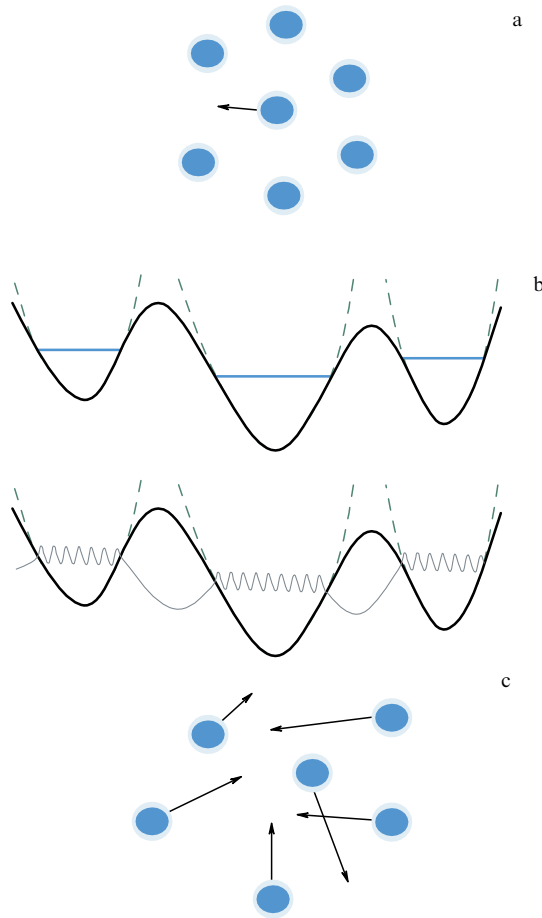


**Figure 33.** Illustration of genesis of zero-point energy of atoms. (a) In a condensed medium, potential relief of environment leads to a ‘cage’ effect and the appearance of zero-point energy due to Heisenberg uncertainty relation; (b) zero-point energy corresponds to lowest energy levels in potential wells created by immediate environment. Conventional wave functions of particles with overlap due to tunneling at low temperatures are also shown. (c) For rarefied gases, there is no continuous potential relief; potential differs from zero only in small neighborhood near the particles. Zero-point energy can be arbitrarily small.

the average interparticle distance  $K^* \approx \pi/a$ , and the momentum can be accordingly estimated as  $P^* \approx \hbar\pi/a$ . Hence, in a condensed medium at arbitrarily low temperatures, a particle cannot have a de Broglie wavelength greater than  $L^* = 2\pi\hbar/P^* \approx 2a$ . Recall that  $L^* \approx 1.3a$  in superfluid helium. In rarefied gases, on the other hand, particles are not in potential wells, and interparticle interaction is significant only in a small region near the particles during their collisions (Fig. 33c). The zero-point energy of particles in such a gas can be arbitrarily small, and the de Broglie wavelength is determined by the temperature and can be arbitrarily large. If the average distance between particles is  $l \gg a$ , where  $a$  is the size of an atom (determined by the effective scattering cross section), then the particle mean free path is  $l^* \approx l^3/a^2$ . Just this  $l^*$  should be considered the coordinate uncertainty in the Heisenberg relation, and the zero-point kinetic energy can be arbitrarily small. As a result, in an ensemble of ultracold atoms, the de Broglie wavelength is determined by the temperature and can exceed the average interparticle distance by orders of magnitude. The majority of atoms can then be in the Bose condensate state with zero momentum. Such atoms share a common wave function, and

their indistinguishability no longer requires a physical exchange of particles, as in the case of liquid helium.

Such fundamental differences between a gas of cold atoms and liquid helium once again cast doubt on the usefulness of the concept of a conventional Bose condensate as applied to liquid superfluid helium. Recall that estimates of the fraction of atoms in a Bose condensate at low pressures and at pressures of 20–25 bar differ by a factor of three (see Fig. 29). Some simple estimates are possible. The bulk compression modulus can be determined from data on the speed of sound and the density of superfluid helium. The speed of sound in helium increases under pressure by approximately 50% (from 230 to 350 m s<sup>−1</sup>) [47]. The density increases by approximately 20% (from 140 to 170 kg m<sup>−3</sup>). The bulk compression modulus increases by a factor of three: from 70 bar at atmospheric pressure to 200–220 bar at a pressure of 24 bar. The derivative of the bulk modulus with respect to pressure has the value  $B'_p \approx 6$ , typical of inert liquids. Such a significant increase in the speed of sound and the modulus should lead to a corresponding increase in the Debye temperature and zero-point energy. Indeed, indirect experimental data show that the zero-point kinetic energy of helium atoms increases from 14 to 19 K [76, 77]. When analyzing the dynamical structure factor in order to estimate the fraction of atoms in the condensate, the component associated with zero-momentum atoms is considered. Obviously, with an increase in zero-point kinetic energy, the effective fraction of ‘slow’ atoms also decreases several-fold. This could be the reason for the significant decrease in the effective fraction of atoms in the condensate as the pressure increases. We note that the authors of [77] also associate the increase in the zero-point kinetic energy with a decrease in the condensate fraction, but for other reasons and considerations.

The importance of the excitation spectrum features for understanding the nature of superfluidity has not yet been realized in analyzing possible superfluidity in the solid state (‘supersolidity’). The excitation spectra for crystalline helium at temperatures above 1 K are typical of anharmonic crystals. The spectra are of course damped less than in a normal liquid, but greater than in the superfluid phase. As in ordinary crystals, there are no ‘real’ rotons in the excitation spectrum of crystalline helium, and, to describe its heat capacity, it suffices to take only the phonons inside the first Brillouin zone into account. There is still no consensus among physicists regarding the possible superfluidity of solid helium at ultralow temperatures. However, it is certain that the excitation spectra in a hypothetical superfluid state of the solid phase should be greatly modified. Obviously, direct experimental studies of the solid state at ultralow temperatures are needed.

To summarize this section, we can conclude that it is apparently impossible to smoothly move from the weakly nonideal gas model to the liquid model with a sufficiently strong interparticle interaction. The picture of correlated monochromatic flickering of helium atoms with high kinetic energy still awaits an appropriate theoretical description.

## 9. Conclusions

In this mini review, we very briefly discussed some issues associated with excitations in disordered media. In our opinion, this field is among the most interesting and at the same time among the least studied in condensed matter

physics. Many theoretical concepts, including the theory of random matrices, remained outside this review. We also barely touched on the extensive experimental and theoretical fields of physics of so-called ‘boson peaks’ in glasses or the model of two-level systems. We also note that, although the list of references is far from complete, the interested reader can easily follow the cross references. Readers interested in the history of the discovery of superfluidity should of course familiarize themselves with the pioneering works of Kapitza, Pomeranchuk, Allen, and others [78–80]. The current state of many issues related to the physics of superfluidity is presented in monograph [81]. The details of the discovery of superfluidity in helium 3 are well described in [82].<sup>2</sup>

The main goal of this review was a detailed comparison of the spectra of collective excitations in ordinary liquids and in superfluid helium. In the course of the presentation, partly tied to the historic sequence of studies, we had to reverse our initial conclusions to the opposite several times. It seemed at first that the excitation spectra in superfluid helium and ordinary liquids have nothing in common. Then, we came to the conclusion that the features of these spectra are almost identical, with minor differences. The final verdict is that, despite some similarities, there are significant and highly important differences.

Despite the great progress in both experimental studies and theoretical models of superfluid helium, it is still impossible to quantitatively describe all the features of the spectrum of collective excitations in the superfluid state. The concept of a Bose condensate in superfluid helium also remains controversial in many ways. Arguably, in the 80 years that have passed since Landau’s first papers, physicists have not advanced very far in understanding the nature of superfluidity. It can only be stated unequivocally that the primary cause of helium’s behavior is a ‘somehow’ correlated state of atoms and a linear, weakly damped part of the spectrum of collective excitations. The role of the large zero-point energy of helium atoms in the superfluid state remains not fully understood or appreciated.

Progress has been more significant in the area of a theoretical description of the spectra of collective excitations in ordinary liquids. The similarity of the spectra in liquids and crystals, associated with the presence of short-range order in liquids, agrees well with the description of liquids following Frenkel [13, 83]. But problems remain even here, because eigenexcitations differ greatly from harmonic plane waves at high frequencies. The excitation spectra in both ordinary and superfluid liquids determine their thermodynamic properties. In this field, too, a number of interesting and important results have been obtained in recent years. But, in general, there are more questions than answers in the physics of collective excitations in disordered systems. As an experimentalist trying to reason, I see the goal of this review as pointing out low-hanging fruit in this field to ‘genuine’ good theorists.

**Acknowledgments.** The author is grateful to V.P. Mineev, [K. (Kostya) Trachenko], O.B. Tsiok, V.N. Ryzhov, M.V. Sadovskii, and P.I. Arseev for the useful discussions of this work and to I.V. Danilov for invaluable assistance in preparing illustrations for the paper and for its careful reading. The author is also grateful to S.M. Stishov for

many years of discussions of issues related to the physics of liquids. The work was carried out with the financial support of the Russian Science Foundation (24-12-00037).

## References

1. Maradudin A A, Montroll E W, Weiss G H *Theory of Lattice Dynamics in the Harmonic Approximation* (New York: Academic Press, 1963); Translated into Russian: *Dinamicheskaya Teoriya Kristallicheskoj Reshetki v Garmonicheskom Priblizhenii* (Moscow: Mir, 1965)
2. Landau L D *J. Phys. USSR* **5** 71 (1941); *Zh. Eksp. Teor. Fiz.* **11** 592 (1941)
3. Bijl A *Physica* **7** 869 (1940)
4. Landau L D *J. Phys. USSR* **11** 91 (1947)
5. Henshaw D G *Phys. Rev. Lett.* **1** 127 (1958)
6. Yarnell J L et al. *Phys. Rev. Lett.* **1** 9 (1958)
7. Yakovlev D G *Phys. Usp.* **44** 823 (2001); *Usp. Fiz. Nauk* **171** 866 (2001)
8. Glyde H R *Rep. Prog. Phys.* **81** 014501 (2018)
9. Trachenko K *Theory of Liquids: From Excitations to Thermodynamics* (Cambridge: Cambridge Univ. Press, 2023) <https://doi.org/10.1017/9781009355483>
10. Scopigno T, Ruocco G, Sette F *Rev. Mod. Phys.* **77** 881 (2005)
11. Trachenko K, Brazhkin V V *Rep. Prog. Phys.* **79** 016502 (2016)
12. Brazhkin V V *Phys. Usp.* **64** 1049 (2021); *Usp. Fiz. Nauk* **191** 1107 (2021)
13. Brazhkin V V et al. *Phys. Usp.* **55** 1061 (2012); *Usp. Fiz. Nauk* **182** 1137 (2012)
14. Brazhkin V V, Trachenko K *Phys. Today* **65** (11) 68 (2012)
15. Brazhkin V V, Trachenko K *J. Non-Cryst. Solids* **407** 149 (2015)
16. Ashcroft N W, Mermin N D *Solid State Physics* (New York: Holt, Rinehart and Winston, 1976); Translated into Russian: *Fizika Tverdogo Tela* (Moscow: Mir, 1979)
17. Malinovskii V K, Novikov V N, Sokolov A P *Phys. Usp.* **36** 440 (1993); *Usp. Fiz. Nauk* **163** (5) 119 (1993)
18. Allen P B et al. *Philos. Mag.* **B 79** 1715 (1999)
19. Keyes T J *J. Chem. Phys.* **101** 5081 (1994)
20. Lin Sh-T, Blanco M, Goddard W A (III) *J. Chem. Phys.* **119** 11792 (2003)
21. Lifshitz E M *Usp. Fiz. Nauk* **34** 512 (1948)
22. Andronikashvili É L *Sov. Phys. Usp.* **3** 888 (1961); *Usp. Fiz. Nauk* **72** 697 (1960)
23. Khalatnikov I M *Teoriya Sverkhtekuchesti* (Theory of Superfluidity) (Moscow: Nauka, 1971)
24. Yarnell J L et al. *Phys. Rev.* **113** 1379 (1959)
25. Cocking S J *Adv. Phys.* **16** 189 (1967)
26. Dasannacharya B A, Rao K R *Phys. Rev.* **137** A417 (1965)
27. Teixeira J et al. *Phys. Rev. Lett.* **54** 2681 (1985)
28. Hosokawa S Z *Phys. Chem.* **235** 99 (2021)
29. Egelstaff P A, in *Neutron Scattering* (Methods in Experimental Physics, Vol. 23, Pt. B, Eds D L Price, K Sköld) (San Diego: Academic Press, 1987) pp. 405–470, [https://doi.org/10.1016/S0076-695X\(08\)60574-8](https://doi.org/10.1016/S0076-695X(08)60574-8)
30. Cunsolo A et al. *J. Chem. Phys.* **114** 2259 (2001)
31. Gorelli F et al. *Phys. Rev. Lett.* **97** 245702 (2006)
32. Giordano V M, Monaco G *Proc. Natl. Acad. Sci. USA* **107** 21985 (2010)
33. Inui M et al. *J. Phys. Condens. Matter* **33** 475101 (2021)
34. Kajihara Y et al. *J. Phys. Conf. Ser.* **98** 022001 (2008)
35. Scopigno T et al. *Phys. Rev. B* **64** 012301 (2001)
36. Grest G S, Nagel S R, Rahman A *Phys. Rev. Lett.* **49** 1271 (1982)
37. Ruocco G, Sette F *Condens. Matter Phys.* **11** 29–46 (2008) <https://doi.org/10.5488/CMP.11.1.29>
38. Brazhkin V V, Danilov I V, Tsiok O B *JETP Lett.* **117** 834 (2023); *Pis'ma Zh. Eksp. Teor. Fiz.* **117** 840 (2023)
39. Brazhkin V V et al. *Phys. Rev. E* **85** 031203 (2012)
40. Cockrell C, Brazhkin V V, Trachenko K *Phys. Rep.* **941** 1 (2021)
41. Krausser J “Non-affine lattice dynamics of disordered solids,” PhD Thesis (Cambridge: Univ. of Cambridge, 2017) <https://doi.org/10.17863/CAM.28051>; <https://www.repository.cam.ac.uk/handle/1810/280686>
42. Hosokawa S et al. *J. Phys. Condens. Matter* **25** 112101 (2013)

<sup>2</sup> The author is grateful to the referee for pointing out these important studies.

43. Kryuchkov N P et al. *Sci. Rep.* **9** 10483 (2019)
44. del Rio B G, González L E *Phys. Rev. B* **95** 224201 (2017)
45. Bryk T et al. *J. Phys. Condens. Matter* **32** 184002 (2020)
46. Jakse N, Bryk T J. *Chem. Phys.* **151** 034506 (2019)
47. Godfrin H et al. *Phys. Rev. B* **103** 104516 (2021)
48. Pitaevskii L P *Sov. Phys. JETP* **9** 830 (1959); *Zh. Eksp. Teor. Fiz.* **36** 1168 (1959)
49. Fåk B, Scherm R *Physica B* **197** 206 (1994)
50. Glyde H R et al. *Europhys. Lett.* **43** 422 (1998)
51. Svensson E C et al. *Phys. Rev. B* **21** 3638 (1980)
52. Barker J A, Henderson D *Rev. Mod. Phys.* **48** 587 (1976)
53. Wang L et al. *Phys. Rev. E* **95** 032116 (2017)
54. Kryuchkov N P et al. *Phys. Rev. Lett.* **125** 125501 (2020)
55. NIST Chemistry WebBook. Thermophysical Properties of Fluid Systems, <https://webbook.nist.gov/chemistry/fluid/>
56. Andreev A F *JETP Lett.* **28** 556 (1978); *Pis'ma Zh. Eksp. Teor. Fiz.* **28** 603 (1978)
57. Strongin M, Zimmerman G O, Fairbank H A *Phys. Rev.* **128** 1983 (1962)
58. Roberts T R, Sydoriak S G *Phys. Rev.* **98** 1672 (1955)
59. Alvesalo T A, Haavasoja T, Manninen M T *J. Low Temp. Phys.* **45** 373 (1981)
60. Alberghamo F et al. *Phys. Rev. Lett.* **100** 239602 (2008)
61. Stishov S M *Phys. Usp.* **67** 338 (2024); *Usp. Fiz. Nauk* **194** 360 (2024)
62. Enkovich P V et al. *Phys. Rev. B* **93** 014308 (2016)
63. Roberts Th R, Sydoriak S G *Phys. Fluids* **3** 895 (1960)
64. Suemitsu M, Sawada Y *Phys. Lett. A* **71** 71 (1979)
65. Babaev E, Sudbø A, Ashcroft N W *Nature* **431** 666 (2004)
66. Leggett A J *Quantum Liquids: Bose Condensation and Cooper Pairing in Condensed-Matter Systems* (Oxford: Oxford Univ. Press, 2008)
67. Zloshchastiev K G *Eur. Phys. J. B* **85** 273 (2012)
68. Campbell C E, Krotscheck E, Lichtenegger T *Phys. Rev. B* **91** 184510 (2015)
69. Ferré G, Boronat J *Phys. Rev. B* **93** 104510 (2016)
70. Beauvois K et al. *Phys. Rev. B* **97** 184520 (2018)
71. Fåk B *Phys. Rev. Lett.* **109** 155305 (2012)
72. Trachenko K J. *Phys. Condens. Matter* **35** 085101 (2023)
73. London F *Nature* **141** 643 (1938)
74. Bogolubov N N *Izv. Akad. Nauk SSSR Ser. Fiz.* **11** (1) 77 (1947); *Usp. Fiz. Nauk* **93** 552 (1967); *J. Phys. USSR* **11** 23 (1947)
75. Leggett A J *Science* **319** 1203 (2008)
76. Diallo S O et al. *Phys. Rev. B* **85** 140505 (2012)
77. Glyde H R et al. *Phys. Rev. B* **84** 184506 (2011)
78. Kapitza P *Nature* **141** 74 (1938)
79. Pomeranchuk I Ya *Zh. Eksp. Teor. Fiz.* **20** 919 (1950)
80. Allen J F, Misener A D *Nature* **142** 643 (1938)
81. Slenczka A, Toennies J P (Eds) *Molecules in Superfluid Helium Nanodroplets. Spectroscopy, Structure, and Dynamics* (Topics in Applied Physics, Vol. 145) (Cham: Springer, 2022) <https://doi.org/10.1007/978-3-030-94896-2>
82. Dobbs E R *Phys. Blätter* **32** 591 (1976)
83. Frenkel O *Kinetic Theory of Liquids* (Oxford: The Clarendon Press, 1946); Translated from Russian: *Kineticheskaya Teoriya Zhidkosti* (Leningrad: Nauka, 1975)